Deformable Models in Medical Image Analysis: A Survey

Tim McInerney[1] and Demetri Terzopoulos[2,3]
[1]Department of Computer Science, Ryerson University, Toronto, ON, Canada M5B 2K3
[2]Computer Science Department, University of California, Los Angeles, CA 90095, USA
[3]Department of Computer Science, University of Toronto, Toronto, ON, Canada M5S 3H5

Abstract

This article surveys deformable models, a promising and vigorously researched computer-assisted medical image analysis technique. Among model-based techniques, deformable models offer a unique and powerful approach to image analysis that combines geometry, physics, and approximation theory. They have proven to be effective in segmenting, matching, and tracking anatomic structures by exploiting (bottom-up) constraints derived from the image data together with (top-down) knowledge about the location, size, and shape of these structures. Deformable models are capable of accommodating the significant variability of biological structures over time and across different individuals. Furthermore, they support highly intuitive interaction mechanisms that, when necessary, allow medical scientists and practitioners to bring their expertise to bear on the model-based image interpretation task. This article reviews the rapidly expanding body of work on the development and application of deformable models to problems of fundamental importance in medical image analysis, including segmentation, shape representation, matching, and motion tracking.

Key Words: Deformable Models, Shape Modeling, Segmentation, Matching, Motion Tracking.

Publication History

This survey is an updated version of the article first published as

> "Deformable models in medical image analysis: A survey," T. McInerney, D. Terzopoulos, *Medical Image Analysis*, **1**(2), 1996, 91–108,

which was reprinted in the volume

> *Deformable Models in Medical Image Analysis*, A. Singh, D. Goldgof, D. Terzopoulos (eds.), IEEE Computer Society Press, Los Alamitos, CA, 1998, 2–19,

and as the chapter

> "Deformable Models," T. McInerney, D. Terzopoulos, in *Handbook of Medical Imaging: Processing and Analysis*, I. Bankman (ed.), Academic Press, San Diego, 2000, Ch. 8, 127–145.

The second edition of the chapter,

> "Deformable Models," T. McInerney, D. Terzopoulos, in *Handbook of Medical Image Processing and Analysis (2nd Edition)*, I. Bankman (ed.), Academic Press, San Diego, 2008, Ch. 8, 145–166,

is close to the present form.

Contents

Abstract 1

Contents 2

1 Introduction 3

2 Mathematical Foundations of Deformable Models 4
- 2.1 Energy-Minimizing Deformable Models . . . 4
- 2.2 Dynamic Deformable Models . . . 6
- 2.3 Discretization and Numerical Simulation . . . 6
- 2.4 Probabilistic Deformable Models . . . 7

3 Medical Image Analysis with Deformable Models 8
- 3.1 Image Segmentation with Deformable Curves . . . 8
- 3.2 Volume Image Segmentation with Deformable Surfaces . . . 11
- 3.3 Incorporating Knowledge . . . 12
- 3.4 Matching . . . 14
- 3.5 Motion Tracking and Analysis . . . 16

4 Discussion 20
- 4.1 Autonomy vs Control . . . 20
- 4.2 Generality vs Specificity . . . 21
- 4.3 Compactness vs Geometric Coverage vs Topological Flexibility . . . 21
- 4.4 Curve vs Surface vs Solid Models . . . 21
- 4.5 Accuracy and Quantitative Power . . . 22
- 4.6 Robustness . . . 22
- 4.7 Lagrangian vs Eulerian Deformable Models . . . 23

5 Conclusion 23

Acknowledgements 24

References 35

Index 35

1 Introduction

The rapid development and proliferation of medical imaging technologies is revolutionizing medicine. Medical imaging allows scientists and physicians to glean potentially life-saving information by peering noninvasively into the human body. The role of medical imaging has expanded beyond the simple visualization and inspection of anatomic structures. It has become a tool for surgical planning and simulation, intra-operative navigation, radiotherapy planning, and for tracking the progress of disease. For example, ascertaining the detailed shape and organization of anatomic structures enables a surgeon preoperatively to plan an optimal approach to some target structure. In radiotherapy, medical imaging allows the delivery of a necrotic dose of radiation to a tumor with minimal collateral damage to healthy tissue.

With medical imaging playing an increasingly prominent role in the diagnosis and treatment of disease, the medical image analysis community has become preoccupied with the challenging problem of extracting, with the assistance of computers, clinically useful information about anatomic structures imaged through CT, MR, PET, and other modalities [Stytz *et al.*, 1991; Robb, 1994; Höhne & Kikinis, 1996; Ayache, 1995a; Bizais *et al.*, 1995; Duncan & Gindi, 1997; Ayache, 1995b; Troccaz *et al.*, 1997; Wells *et al.*, 1998; Duncan & Ayache, 2000]. Although modern imaging devices provide exceptional views of internal anatomy, the use of computers to quantify and analyze the embedded structures with accuracy and efficiency is limited. Accurate, repeatable, quantitative data must be efficiently extracted in order to support the spectrum of biomedical investigations and clinical activities from diagnosis, to radiotherapy, to surgery.

For example, segmenting structures from medical images and reconstructing a compact geometric representation of these structures is difficult due to the sheer size of the datasets and the complexity and variability of the anatomic shapes of interest. Furthermore, the shortcomings typical of sampled data, such as sampling artifacts, spatial aliasing, and noise, may cause the boundaries of structures to be indistinct and disconnected. The challenge is to extract boundary elements belonging to the same structure and integrate these elements into a coherent and consistent model of the structure. Traditional low-level image processing techniques which consider only local information can make incorrect assumptions during this integration process and generate infeasible object boundaries. As a result, these model-free techniques usually require considerable amounts of expert intervention. Furthermore, the subsequent analysis and interpretation of the segmented objects is hindered by the pixel- or voxel-level structure representations generated by most image processing operations.

This chapter surveys deformable models, one of the most intensively researched model-based approaches to computer-assisted medical image analysis. The widely recognized potency of deformable models stems from their ability to segment, match, and track images of anatomic structures by exploiting (bottom-up) constraints derived from the image data together with (top-down) knowledge about the location, size, and shape of these structures. Deformable models are capable of accommodating the often significant variability of biological structures over time and across different individuals. Furthermore, deformable models support highly intuitive interaction mechanisms that allow medical scientists and practitioners to bring their expertise to bear on the model-based image interpretation task when necessary. We will review the basic formulation of deformable models and survey their application to fundamental medical image analysis problems, including segmentation, shape representation, matching, and motion tracking. The chapter is an updated version of [McInerney & Terzopoulos, 1996] (see also the compilation [Singh *et al.*, 1998]).

2 Mathematical Foundations of Deformable Models

The classical mathematical foundations of deformable models represent the confluence of geometry, physics, and approximation theory. Geometry serves to represent object shape, physics imposes constraints on how the shape may vary over space and time, and optimal approximation theory provides the formal underpinnings of mechanisms for fitting the models to measured data.

Deformable model geometry usually permits broad shape coverage by employing geometric representations that involve many degrees of freedom, such as splines . The model remains manageable, however, because the degrees of freedom are generally not permitted to evolve independently, but are governed by physical principles that bestow intuitively meaningful behavior upon the geometric substrate. The name "deformable models" stems primarily from the use of elasticity theory at the physical level, generally within a Lagrangian dynamics setting. The physical interpretation views deformable models as elastic bodies which respond naturally to applied forces and constraints. Typically, deformation energy functions defined in terms of the geometric degrees of freedom are associated with the deformable model. The energy grows monotonically as the model deforms away from a specified natural or "rest shape" and often includes terms that constrain the smoothness or symmetry of the model. In the Lagrangian setting, the deformation energy gives rise to elastic forces internal to the model. Taking a physics-based view of classical optimal approximation, external potential energy functions are defined in terms of the data of interest to which the model is to be fitted. These potential energies give rise to external forces which deform the model such that it fits the data.

Deformable curve, surface, and solid models gained popularity after they were proposed for use in computer vision [Terzopoulos *et al.*, 1988] and computer graphics [Terzopoulos & Fleischer, 1988] in the mid 1980's. Terzopoulos introduced the theory of continuous (multidimensional) deformable models in a Lagrangian dynamics setting [Terzopoulos, 1986a], based on deformation energies in the form of (controlled-continuity) generalized splines [Terzopoulos, 1986b]. Ancestors of the deformable models now in common use include Fischler and Elshlager's spring-loaded templates [1973] and Widrow's rubber mask technique [1973].

The deformable model that has attracted the most attention to date is popularly known as "snakes" [Kass *et al.*, 1988]. Snakes or "active contour models" represent a special case of the general multidimensional deformable model theory [Terzopoulos, 1986a]. We will review their simple formulation in the remainder of this section in order to illustrate with a concrete example the basic mathematical machinery that is present in many deformable models.

Snakes are planar deformable contours that are useful in several image analysis tasks. They are often used to approximate the locations and shapes of object boundaries in images based on the reasonable assumption that boundaries are piecewise continuous or smooth (Fig. 1). In its basic form, the mathematical formulation of snakes draws from the theory of optimal approximation involving functionals.

2.1 Energy-Minimizing Deformable Models

Geometrically, a snake is a parametric contour embedded in the image plane $(x, y) \in \Re^2$. The contour is represented as $\mathbf{v}(s) = (x(s), y(s))^\top$, where x and y are the coordinate functions and $s \in [0, 1]$ is the parametric domain. The shape of the contour subject to an image $I(x, y)$ is dictated by the functional

$$\mathcal{E}(\mathbf{v}) = \mathcal{S}(\mathbf{v}) + \mathcal{P}(\mathbf{v}). \tag{1}$$

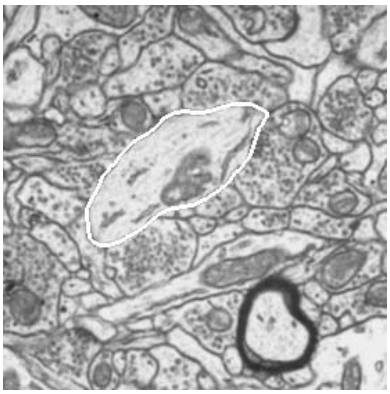

Figure 1: Snake (white) attracted to cell membrane in an EM photomicrograph (from [Carlbom *et al.*, 1994]).

The functional can be viewed as a representation of the energy of the contour and the final shape of the contour corresponds to the minimum of this energy. The first term of the functional,

$$\mathcal{S}(\mathbf{v}) = \int_0^1 w_1(s) \left| \frac{\partial \mathbf{v}}{\partial s} \right|^2 + w_2(s) \left| \frac{\partial^2 \mathbf{v}}{\partial s^2} \right|^2 ds, \tag{2}$$

is the internal deformation energy. It characterizes the deformation of a stretchy, flexible contour. Two physical parameter functions dictate the simulated physical characteristics of the contour: $w_1(s)$ controls the "tension" of the contour while $w_2(s)$ controls its "rigidity".[1] The second term in (1) couples the snake to the image. Traditionally,

$$\mathcal{P}(\mathbf{v}) = \int_0^1 P(\mathbf{v}(s)) ds, \tag{3}$$

where $P(x, y)$ denotes a scalar potential function defined on the image plane. To apply snakes to images, external potentials are designed whose local minima coincide with intensity extrema, edges, and other image features of interest. For example, the contour will be attracted to intensity edges in an image $I(x, y)$ by choosing a potential $P(x, y) = -c|\nabla[G_\sigma * I(x, y)]|$, where c controls the magnitude of the potential, ∇ is the gradient operator, and $G_\sigma * I$ denotes the image convolved with a (Gaussian) smoothing filter whose characteristic width σ controls the spatial extent of the local minima of P.

In accordance with the calculus of variations, the contour $\mathbf{v}(s)$ which minimizes the energy $\mathcal{E}(\mathbf{v})$ must satisfy the Euler-Lagrange equation

$$-\frac{\partial}{\partial s}\left(w_1 \frac{\partial \mathbf{v}}{\partial s}\right) + \frac{\partial^2}{\partial s^2}\left(w_2 \frac{\partial^2 \mathbf{v}}{\partial s^2}\right) + \nabla P(\mathbf{v}(s,t)) = \mathbf{0}. \tag{4}$$

This vector-valued partial differential equation expresses the balance of internal and external forces when the contour rests at equilibrium. The first two terms represent the internal stretching and bending forces, respectively, while the third term represents the external forces that couple the snake to the image data. The usual approach to solving (4) is through the application of numerical algorithms (Sec. 2.3).

[1] The values of the non-negative functions $w_1(s)$ and $w_2(s)$ determine the extent to which the snake can stretch or bend at any point s on the snake. For example, increasing the magnitude of $w_1(s)$ increases the "tension" and tends to eliminate extraneous loops and ripples by reducing the length of the snake. Increasing $w_2(s)$ increases the bending "rigidity" of the snake and tends to make the snake smoother and less flexible. Setting the value of one or both of these functions to zero at a point s permits discontinuities in the contour at s.

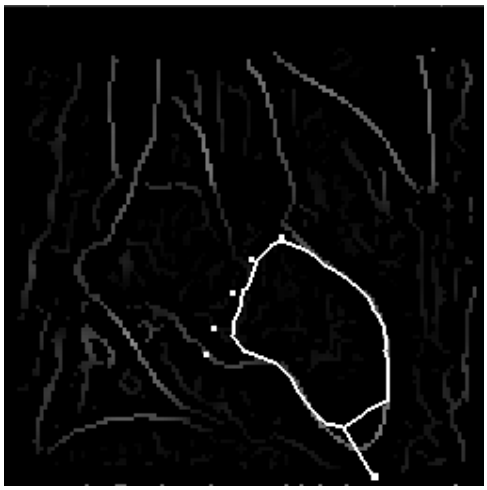

Figure 2: Snake deforming towards high gradients in a processed cardiac image, influenced by "pin" points and an interactive "spring" which pulls the contour towards an edge (from [McInerney & Terzopoulos, 1995a]).

2.2 Dynamic Deformable Models

While it is natural to view energy minimization as a static problem, a potent approach to computing the local minima of a functional such as (1) is to construct a dynamical system that is governed by the functional and allow the system to evolve to equilibrium. The system may be constructed by applying the principles of Lagrangian mechanics. This leads to dynamic deformable models that unify the description of shape and motion, making it possible to quantify not just static shape, but also shape evolution through time. Dynamic models are valuable for medical image analysis, since most anatomical structures are deformable and continually undergo nonrigid motion *in vivo*. Moreover, dynamic models exhibit intuitively meaningful physical behaviors, making their evolution amenable to interactive guidance from a user (Fig. 2).

A simple example is a dynamic snake which can be represented by introducing a time-varying contour $\mathbf{v}(s,t) = (x(s,t), y(s,t))^\top$ with a mass density $\mu(s)$ and a damping density $\gamma(s)$. The Lagrange equations of motion for a snake with the internal energy given by (2) and external energy given by (3) is

$$\mu \frac{\partial^2 \mathbf{v}}{\partial t^2} + \gamma \frac{\partial \mathbf{v}}{\partial t} - \frac{\partial}{\partial s}\left(w_1 \frac{\partial \mathbf{v}}{\partial s}\right) + \frac{\partial^2}{\partial s^2}\left(w_2 \frac{\partial^2 \mathbf{v}}{\partial s^2}\right) = -\nabla P(\mathbf{v}(s,t)). \tag{5}$$

The first two terms on the left hand side of this partial differential equation represent inertial and damping forces. Referring to (4), the remaining terms represent the internal stretching and bending forces, while the right hand side represents the external forces. Equilibrium is achieved when the internal and external forces balance and the contour comes to rest (i.e., $\partial \mathbf{v}/\partial t = \partial^2 \mathbf{v}/\partial t^2 = 0$), which yields the equilibrium condition (4).

2.3 Discretization and Numerical Simulation

In order to numerically compute a minimum energy solution, it is necessary to discretize the energy $\mathcal{E}(\mathbf{v})$. The usual approach is to represent the continuous geometric model $\mathbf{v}$ in terms of linear combinations of local-support or global-support basis functions. Finite elements [Zienkiewicz &

Taylor, 1989], finite differences [Press *et al.*, 1992], and geometric splines [Farin, 1993] are local representation methods, whereas Fourier bases [Ballard & Brown, 1982] are global representation methods. The continuous model $\mathbf{v}(s)$ is represented in discrete form by a vector $\mathbf{u}$ of shape parameters associated with the basis functions. The discrete form of energies such as $\mathcal{E}(\mathbf{v})$ for the snake may be written as

$$E(\mathbf{u}) = \frac{1}{2}\mathbf{u}^\top \mathbf{K}\mathbf{u} + \mathrm{P}(\mathbf{u}) \tag{6}$$

where $\mathbf{K}$ is called the *stiffness matrix*, and $\mathrm{P}(\mathbf{u})$ is the discrete version of the external potential. The minimum energy solution results from setting the gradient of (6) to $\mathbf{0}$, which is equivalent to solving the set of algebraic equations

$$\mathbf{K}\mathbf{u} = -\nabla \mathrm{P} = \mathbf{f} \tag{7}$$

where $\mathbf{f}$ is the generalized external force vector.

The discretized version of the Lagrangian dynamics equation (5) may be written as a set of second order ordinary differential equations for $\mathbf{u}(t)$:

$$\mathbf{M}\ddot{\mathbf{u}} + \mathbf{C}\dot{\mathbf{u}} + \mathbf{K}\mathbf{u} = \mathbf{f}, \tag{8}$$

where $\mathbf{M}$ is the mass matrix and $\mathbf{C}$ is a damping matrix. The time derivatives in (5) are approximated by finite differences and explicit or implicit numerical time integration methods are applied to simulate the resulting system of ordinary differential equations in the shape parameters $\mathbf{u}$.

2.4 Probabilistic Deformable Models

An alternative view of deformable models emerges from casting the model fitting process in a probabilistic framework, often taking a Bayesian approach. This permits the incorporation of prior model and sensor model characteristics in terms of probability distributions. The probabilistic framework also provides a measure of the uncertainty of the estimated shape parameters after the model is fitted to the image data [Szeliski, 1990].

Let $\mathbf{u}$ represent the deformable model shape parameters with a prior probability $p(\mathbf{u})$ on the parameters. Let $p(I|\mathbf{u})$ be the imaging (sensor) model—the probability of producing an image I given a model $\mathbf{u}$. Bayes' theorem

$$p(\mathbf{u}|I) = \frac{p(I|\mathbf{u})p(\mathbf{u})}{p(I)} \tag{9}$$

expresses the posterior probability $p(\mathbf{u}|I)$ of a model given the image, in terms of the imaging model and the prior probabilities of model and image.

It is easy to convert the internal energy measure (2) of the deformable model into a prior distribution over expected shapes, with lower energy shapes being the more likely. This is achieved using a Boltzman (or Gibbs) distribution of the form

$$p(\mathbf{u}) = \frac{1}{Z_s}\exp(-S(\mathbf{u})), \tag{10}$$

where $S(\mathbf{u})$ is the discretized version of $\mathcal{S}(\mathbf{v})$ in (2) and Z_s is a normalizing constant (called the partition function). This prior model is then combined with a simple sensor model based on linear measurements with Gaussian noise

$$p(I|\mathbf{u}) = \frac{1}{Z_I}\exp(-\mathrm{P}(\mathbf{u})), \tag{11}$$

where $\mathrm{P}(\mathbf{u})$ is a discrete version of the potential $\mathcal{P}(\mathbf{v})$ in (3), which is a function of the image $I(x, y)$.

Models may be fitted by finding $\mathbf{u}$ which locally maximize $p(\mathbf{u}|I)$ in (9). This is known as the maximum a posteriori (MAP) solution. With the above construction, it yields the same result as minimizing (1), the energy configuration of the deformable model given the image.

The probabilistic framework can be extended by assuming a time-varying prior model, or system model, in conjunction with the sensor model, resulting in a Kalman filter. The system model describes the expected evolution of the shape parameters $\mathbf{u}$ over time. If the equations of motion of the physical snakes model (8) are employed as the system model, the result is a sequential estimation algorithm known as "Kalman snakes" [Terzopoulos & Szeliski, 1992].

3 Medical Image Analysis with Deformable Models

Although originally developed for application to problems in computer vision and computer graphics, the potential of deformable models for use in medical image analysis has been quickly realized. They have been applied to images generated by imaging modalities as varied as X-ray, computed tomography (CT), angiography, magnetic resonance (MR), and ultrasound. Two dimensional and three dimensional deformable models have been used to segment, visualize, track, and quantify a variety of anatomic structures ranging in scale from the macroscopic to the microscopic. These include the brain, heart, face, cerebral, coronary and retinal arteries, kidney, lungs, stomach, liver, skull, vertebra, objects such as brain tumors, a fetus, and even cellular structures such as neurons and chromosomes. Deformable models have been used to track the nonrigid motion of the heart, the growing tip of a neurite, and the motion of erythrocytes. They have been used to locate structures in the brain, and to register images of the retina, vertebra and neuronal tissue.

In the following sections, we review and discuss the application of deformable models to medical image interpretation tasks including segmentation, matching, and motion analysis.

3.1 Image Segmentation with Deformable Curves

The segmentation of anatomic structures—the partitioning of the original set of image points into subsets corresponding to the structures—is an essential first stage of most medical image analysis tasks, such as registration, labeling, and motion tracking. These tasks require anatomic structures in the original image to be reduced to a compact, analytic representation of their shapes. Performing this segmentation manually is extremely labor intensive and time-consuming. A primary example is the segmentation of the heart, especially the left ventricle (LV), from cardiac imagery. Segmentation of the left ventricle is a prerequisite for computing diagnostic information such as ejection-fraction ratio, ventricular volume ratio, heart output, and for wall motion analysis which provides information on wall thickening, etc. [Singh *et al.*, 1993].

Most clinical segmentation is currently performed using manual slice editing. In this scenario, a skilled operator, using a computer mouse or trackball, manually traces the region of interest on each slice of an image volume. Manual slice editing suffers from several drawbacks. These include the difficulty in achieving reproducible results, operator bias, forcing the operator to view each 2D slice separately to deduce and measure the shape and volume of 3D structures, and operator fatigue.

Segmentation using traditional low-level image processing techniques, such as thresholding, region growing, edge detection, and mathematical morphology operations, also requires considerable amounts of expert interactive guidance. Furthermore, automating these model-free approaches is difficult because of the shape complexity and variability within and across individuals. In general, the underconstrained nature of the segmentation problem limits the efficacy of approaches that consider local information only. Noise and other image artifacts can cause incorrect regions or boundary discontinuities in objects recovered by these methods.

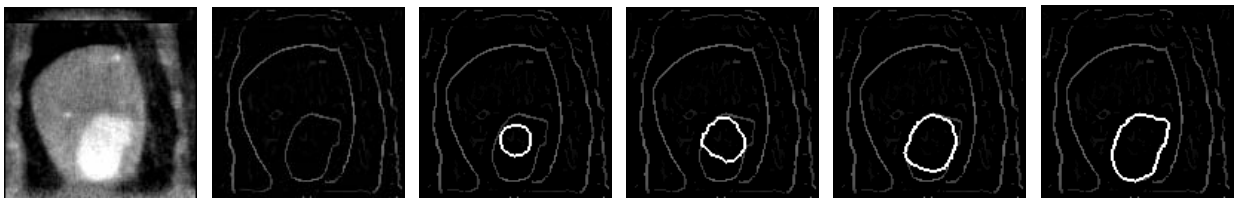

(a) (b) (c) (d) (e) (f)

Figure 3: (a) Intensity CT image slice of canine LV. (b) Edge detected image. (c) Initial snake. (d)-(f) Snake deforming towards LV boundary, driven by "inflation" force. (From [McInerney & Terzopoulos, 1995a].)

A deformable model based segmentation scheme, used in concert with image pre-processing, can overcome many of the limitations of manual slice editing and traditional image processing techniques. These connected and continuous geometric models consider an object boundary as a whole and can make use of prior knowledge of object shape to constrain the segmentation problem. The inherent continuity and smoothness of the models can compensate for noise, gaps and other irregularities in object boundaries. Furthermore, the parametric representations of the models provide a compact, analytical description of object shape. These properties lead to an efficient, robust, accurate and reproducible technique for linking sparse or noisy local image features into a complete and consistent model of the object.

Among the first and primary uses of deformable models in medical image analysis was the application of deformable contour models, such as snakes [Kass *et al.*, 1988], to segment structures in 2D images [Berger, 1990; Cohen, 1991; Ueda & Mase, 1992; Rougon & Prêteux, 1993; Cohen & Cohen, 1993; Leitner & Cinquin, 1993; Carlbom *et al.*, 1994; Gupta *et al.*, 1994; Lobregt & Viergever, 1995; Davatzikos & Prince, 1995; Paulus *et al.*, 1999]. Typically users initialized a deformable model near the object of interest (Fig. 3) and allowed it to deform into place. Users could then exploit the interactive capabilities of these models and manually fine-tune them. Furthermore, once the user is satisfied with the result on an initial image slice, the fitted contour model may then be used as the initial boundary approximation for neighboring slices. These models are then deformed into place and again propagated until all slices have been processed. The resulting sequence of 2D contours can then be connected to form a continuous 3D surface model [Lin & Chen, 1989; Chang *et al.*, 1991; Cohen, 1991; Cohen & Cohen, 1993].

The application of snakes and other similar deformable contour models to extract regions of interest is, however, not without limitations. For example, snakes were designed as interactive models. In non-interactive applications, they must be initialized close to the structure of interest to guarantee good performance. The internal energy constraints of snakes can limit their geometric flexibility and prevent a snake from representing long tube-like shapes and shapes with significant protrusions or bifurcations. Furthermore, the topology of the structure of interest must be known in advance since classical deformable contour models are parametric and are incapable of topological transformations without additional machinery (such as that in T-snakes [McInerney & Terzopoulos, 2000]).

Various methods have been proposed to improve and further automate the deformable contour segmentation process. Cohen and Cohen [1993] used an internal "inflation" force to expand a snakes model past spurious edges towards the real edges of the structure, making the snake less sensitive to initial conditions (inflation forces were also employed in [Terzopoulos *et al.*, 1988]). Amini *et al.* [1990] use dynamic programming to carry out a more extensive search for global minima.

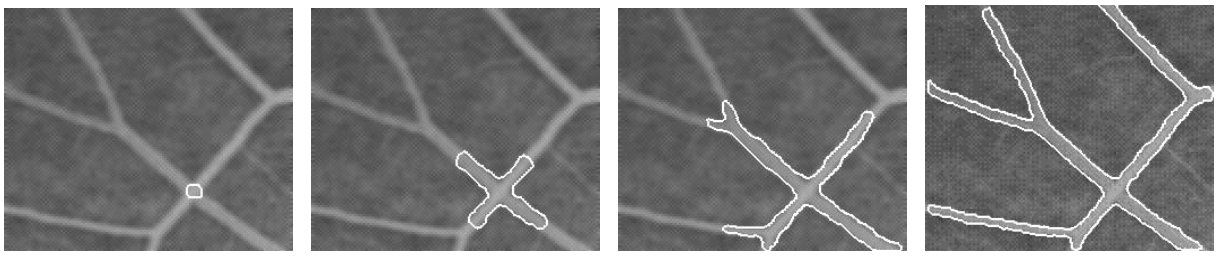

Figure 4: Image sequence of clipped angiogram of retina showing an automatically subdividing snake flowing and branching along a vessel (from [McInerney & Terzopoulos, 1995b]).

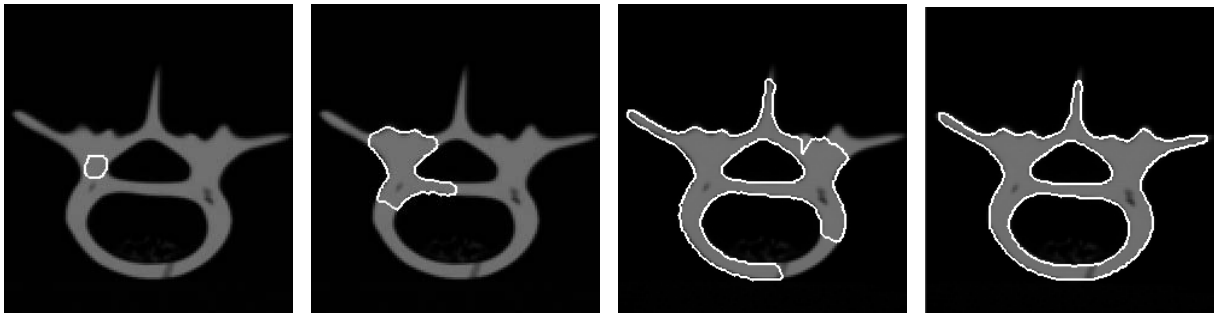

(a) (b) (c) (d)

Figure 5: Segmentation of a cross sectional image of a human vertebra phantom with a topologically adaptable snake (from [McInerney & Terzopoulos, 1995b]). The snake begins as a single closed curve and becomes three closed curves.

Poon *et al.* [1994] and Grzeszczuk and Levin [1997] minimize the energy of active contour models using simulated annealing which is known to give global solutions and allows the incorporation of non-differentiable constraints.

Other researchers [Rougon & Prêteux, 1991; Ivins & Porrill, 1994; Chakraborty & Duncan, 1999; Herlin *et al.*, 1992; Gauch *et al.*, 1994; Mangin *et al.*, 1995; Gunn & Nixon, 1997; Jones & Metaxas, 1997] have integrated region-based information into deformable contour models or used other techniques in an attempt to decrease sensitivity to insignificant edges and initial model placement. For example, Poon *et al.* [1994] use a discriminant function to incorporate region based image features into the image forces of their active contour model. The discriminant function allows the inclusion of additional image features in the segmentation and serves as a constraint for global segmentation consistency (i.e. every image pixel contributes to the discriminant function).

Several researchers [Leitner & Cinquin, 1991; Malladi *et al.*, 1995; Whitaker, 1994; Caselles *et al.*, 1995; Sapiro *et al.*, 1995; Malladi *et al.*, 1996; Caselles *et al.*, 1997; Yezzi *et al.*, 1997; Niessen *et al.*, 1998; Lachaud & Montanvert, 1999; McInerney & Terzopoulos, 2000] have been developing topologically adaptive shape modeling schemes that are not only less sensitive to initial conditions, but also allow a deformable contour or surface model to represent long tube-like shapes or shapes with bifurcations (Fig. 4), and to dynamically sense and change its topology (Fig. 5).

Finally, another development is a snake-like technique known as "live-wire" [Falcão *et al.*, 1998; Barrett & Mortensen, 1996-7]. This semiautomatic boundary tracing technique computes and selects optimal boundaries at interactive rates as the user moves a mouse, starting from a user-specified seed point. When the mouse is moved close to an object edge, a live-wire boundary snaps to, and wraps around the object of interest. The live-wire method has also been combined with snakes, yielding a segmentation tool that exploits the best properties of both techniques [Liang *et al.*, 2006, 1999].

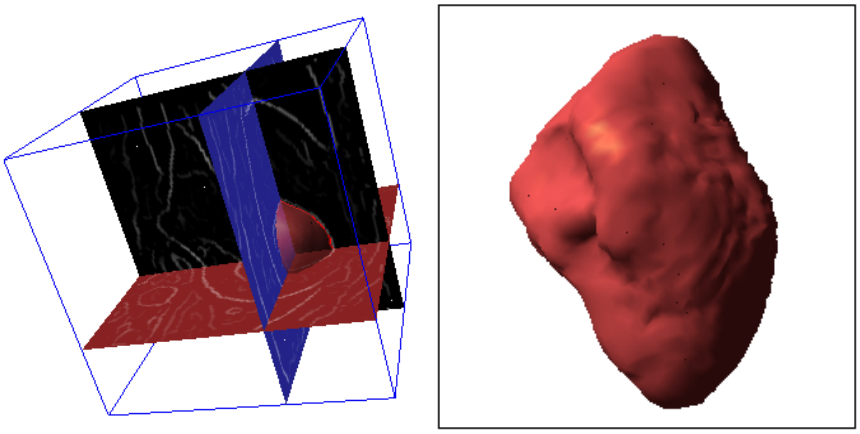

(a) (b)

Figure 6: (a) Deformable "balloon" model embedded in volume image deforming towards LV edges of canine heart (b) Reconstruction of LV. (From [McInerney & Terzopoulos, 1995a].)

3.2 Volume Image Segmentation with Deformable Surfaces

Segmenting 3D image volumes slice by slice using manual slice editing (or image processing techniques) is a laborious process and requires a post-processing step to connect the sequence of 2D contours into a continuous surface. Furthermore, the resulting surface reconstruction can contain inconsistencies or show rings or bands. As described in the previous section, the application of a 2D active contour model to an initial slice and the propagation of the model to neighboring slices can significantly improve the volume segmentation process. However, the use of a true 3D deformable surface model can potentially result in even greater improvements in efficiency and robustness and it also ensures that a globally smooth and coherent surface is produced between image slices.

Deformable surface models in 3D were first used in computer vision [Terzopoulos *et al.*, 1988]. Many researchers have since explored the use of deformable surface models for segmenting structures in medical image volumes. Miller [1991] constructs a polygonal approximation to a sphere and geometrically deforms this "balloon" model until the balloon surface conforms to the object surface in 3D CT data. The segmentation process is formulated as the minimization of a cost function where the desired behavior of the balloon model is determined by a local cost function associated with each model vertex. The cost function is a weighted sum of three terms: a deformation potential that "expands" the model vertices towards the object boundary, an image term that identifies features such as edges and opposes the balloon expansion, and a term that maintains the topology of the model by constraining each vertex to remain close to the centroid of its neighbors.

Cohen and Cohen [1992b; 1993] and McInerney and Terzopoulos [1995a] use finite element and physics-based techniques to implement an elastically deformable cylinder and sphere, respectively. The models are used to segment the inner wall of the left ventricle of the heart from MR or CT image volumes (Fig. 6). These deformable surfaces are based on a thin-plate under tension surface spline, the higher dimensional generalization of equation (2), which controls and constrains the stretching and bending of the surface. The models are fitted to data dynamically by integrating Lagrangian equations of motion through time in order to adjust the deformational degrees of freedom. Furthermore, the finite element method is used to represent the models as a continuous surface in the form of weighted sums of local polynomial basis functions. Unlike Miller's [1991] polygonal model, the finite element method provides an analytic surface representation and the use

of high-order polynomials means that fewer elements are required to accurately represent an object. Pentland and Sclaroff [1991] and Nastar and Ayache [1996] also develop physics-based models but use a reduced modal basis for the finite elements (see Section 3.5).

Staib and Duncan [1992b] describe a 3D surface model used for geometric surface matching to 3D medical image data. The model uses a Fourier parameterization which decomposes the surface into a weighted sum of sinusoidal basis functions. Several different surface types are developed such as tori, open surfaces, closed surfaces and tubes. Surface finding is formulated as an optimization problem using gradient ascent which attracts the surface to strong image gradients in the vicinity of the model. An advantage of the Fourier parameterization is that it allows a wide variety of smooth surfaces to be described with a small number of parameters. That is, a Fourier representation expresses a function in terms of an orthonormal basis and higher indexed basis functions in the sum represent higher spatial variation. Therefore, the series can be truncated and still represent relatively smooth objects accurately.

In a different approach, Szeliski *et al.* [1993] use a dynamic, self-organizing oriented particle system to model surfaces of objects. The oriented particles, which can be visualized as small, flat disks, evolve according to Newtonian mechanics and interact through external and interparticle forces. The external forces attract the particles to the data while interparticle forces attempt to group the particles into a coherent surface. The particles can reconstruct objects with complex shapes and topologies by "flowing" over the data, extracting and conforming to meaningful surfaces. A triangulation is then performed which connects the particles into a continuous global model that is consistent with the inferred object surface.

We have generalized the topologically adaptive snakes (T-snakes) [McInerney & Terzopoulos, 2000] that were cited earlier (Fig. 5), to higher-dimensional surfaces. Known as T-surfaces [McInerney & Terzopoulos, 1999, 1997], these deformable surface models are formulated in terms of an Affine Cell Image Decomposition (ACID), which significantly extends standard deformable surfaces while retaining their interactivity and other desirable properties. In particular, the ACID induces an efficient reparameterization mechanism that enables parametric deformable surfaces to evolve into complex geometries and even modify their topology as necessary in order to segment complex anatomic structures from medical volume images.

Other notable work involving 3D deformable surface models and medical image applications can be found in [Delingette *et al.*, 1992; Whitaker, 1994; Tek & Kimia, 1997; Davatzikos & Bryan, 1995; Neuenschwander *et al.*, 1997; Caselles *et al.*, 1997; Delibasis *et al.*, 1997; Xu & Prince, 1998; Zeng *et al.*, 1998] as well as several models described in the following sections.

3.3 Incorporating Knowledge

In medical images, the general shape, location and orientation of an anatomical structure is known and this knowledge may be incorporated into the deformable model in the form of initial conditions, data constraints, constraints on the model shape parameters, or into the model fitting procedure. The use of implicit or explicit anatomical knowledge to guide shape recovery is especially important for robust automatic interpretation of medical images. For automatic interpretation, it is essential to have a model that not only describes the size, shape, location and orientation of the target object but that also permits expected variations in these characteristics. Automatic interpretation of medical images can relieve clinicians from the labor intensive aspects of their work while increasing the accuracy, consistency, and reproducibility of the interpretations. In this section, and in the following sections on matching and motion tracking, we will describe several deformable model techniques that incorporate prior anatomical knowledge in different ways.

A number of researchers have incorporated knowledge of object shape into deformable models by using deformable shape templates. These models usually use "hand-crafted" global shape pa-

rameters to embody *a priori* knowledge of expected shape and shape variation of the structures and have been used successfully for many applications of automatic image interpretation. The idea of deformable templates can be traced back to the early work on spring loaded templates by Fischler and Elshlager [1973]. An excellent example in computer vision is the work of Yuille *et al.* [1992] who construct deformable templates for detecting and describing features of faces, such as the eye. In an early example from medical image analysis, Lipson *et al.* [1990] note that axial cross sectional images of the spine yield approximately elliptical vertebral contours and consequently extract the contours using a deformable ellipsoidal template. Subsequently, Montagnat and Delingette [1997] used a deformable surface template of the liver to segment it from abdominal CT scans, and a ventricle template to segment the ventricles of the brain from MR images.

Deformable models based on superquadrics are another example of deformable shape templates that are gaining in popularity in medical image research. Superquadrics contain a small number of intuitive global shape parameters that can be tailored to the average shape of a target anatomic structure. Furthermore, the global parameters can often be coupled with local shape parameters such as splines resulting in a powerful hybrid shape representation scheme. For example, Metaxas and Terzopoulos [1993] employ a dynamic deformable superquadric model [Terzopoulos & Metaxas, 1991] to reconstruct and track human limbs from 3D biokinetic data. Their prior models can deform both locally and globally by incorporating the global shape parameters of a superellipsoid with the local degrees of freedom of a membrane spline in a Lagrangian dynamics formulation. The global parameters efficiently capture the gross shape features of the data, while the local deformation parameters reconstruct the fine details of complex shapes. Using Kalman filtering theory, they develop and demonstrate a biokinetic motion tracker based on their deformable superquadric model.

Vemuri and Radisavljevic [1993; 1994] construct a deformable superquadric model in an orthonormal wavelet basis. This multi-resolution basis provides the model with the ability to continuously transform from local to global shape deformations thereby allowing a continuum of shape models to be created and to be represented with relatively few parameters. They apply the model to segment and reconstruct anatomical structures in the human brain from MRI data.

As a final example, Bardinet *et al.* [1996] fit a deformable superquadric to segmented 3D cardiac images and then refine the superquadric fit using a volumetric deformation technique known as free form deformations (FFDs). FFDs are defined by tensor product trivariate splines and can be visualized as a rubber-like box in which the object to be deformed (in this case the superquadric) is embedded. Deformations of the box are automatically transmitted to embedded objects. This volumetric aspect of FFDs allows two superquadric surface models to be simultaneously deformed in order to reconstruct the inner and outer surfaces of the left ventricle of the heart and the volume in between these surfaces. Further examples of deformable superquadrics can be found in [Pentland & Horowitz, 1991; Chen *et al.*, 1994] (see Section 3.5). Further examples of FFD-based (or FFD-like) deformable models for medical image segmentation can be found in [McInerney & Kikinis, 1998; Lötjönen *et al.*, 1999].

Several researchers cast the deformable model fitting process in a probabilistic framework (see Section 2.4) and include prior knowledge of object shape by incorporating prior probability distributions on the shape variables to be estimated [Vemuri & Radisavljevic, 1994; Staib & Duncan, 1992a; Worring *et al.*, 1996; Gee, 1999]. For example, Staib and Duncan [1992a] use a deformable contour model on 2D echocardiograms and MR images to extract the LV of the heart and the corpus callosum of the brain, respectively. This closed contour model is parameterized using an elliptic Fourier decomposition and *a priori* shape information is included as a spatial probability expressed through the likelihood of each model parameter. The model parameter probability distributions are derived from a set of example object boundaries and serve to bias the contour model towards expected or more likely shapes.

Szekely *et al.* [1996] have also developed Fourier parameterized models. Furthermore, they have

added elasticity to their models to create "Fourier snakes" in 2D and elastically deformable Fourier surface models in 3D. By using the Fourier parameterization followed by a statistical analysis of a training set, they define mean organ models and their eigen-deformations. An elastic fit of the mean model in the subspace of eigenmodes restricts possible deformations and finds an optimal match between the model surface and boundary candidates.

Cootes *et al.* [1994] and Hill *et al.* [1993] present a statistically based technique for building deformable shape templates and use these models to segment various organs from 2D and 3D medical images. The statistical parameterization provides global shape constraints and allows the model to deform only in ways implied by the training set. The shape models represent objects by sets of landmark points which are placed in the same way on an object boundary in each input image. For example, to extract the LV from echocardiograms, they choose points around the ventricle boundary, the nearby edge of the right ventricle, and the top of the left atrium. The points can be connected to form a deformable contour. By examining the statistics of training sets of hand-labeled medical images, and using principal components analysis (PCA), a shape model is derived that describes the average positions and the major modes of variation of the object points. New shapes are generated using the mean shape and a weighted sum of the major modes of variation. Object boundaries are then segmented using this *active shape model* by examining a region around each model point to calculate the displacement required to move it towards the boundary. These displacements are then used to update the shape parameter weights. An example of the use of this technique for segmenting MR brain images can be found in [Duta & Sonka, 1998].

An extreme example of incorporating prior knowledge, aspiring toward fully automated medical image segmentation, is *deformable organisms* [McInerney *et al.*, 2002; Hamarneh *et al.*, 2001]. This recent paradigm for automatic image analysis combines deformable models and concepts from artificial life modeling. The goal is to incorporate and exploit all the available prior knowledge and global contextual information in any specific medical image analysis task. Analogous to natural organisms capable of voluntary movement, deformable organisms possess deformable bodies with distributed sensors, as well as (rudimentary) brains with motor, perception, behavior, and cognition centers. Deformable organisms are perceptually aware of the image analysis process. Their behaviors, which manifest themselves in voluntary movement and body shape alteration, are based upon sensed image features, stored structural knowledge, and a cognitive plan. The organism framework separates global top-down, model-fitting control functionality from the local, bottom-up, feature integration functionality. This separation enables the definition of model-fitting controllers or 'brains' in terms of the high-level structural features of objects of interest, rather than the low-level image features. The result is an 'intelligent agent' that is continuously 'aware' of the progress of the segmentation process, allowing it to apply prior knowledge about target objects in a deliberative manner (Fig. 7). 3D physics-based deformable organisms have recently been developed [McIntosh & Hamarneh, 2006b] and software is available [McIntosh & Hamarneh, 2006a].

3.4 Matching

Matching of regions in images can be performed between the representation of a region and a model (labeling) or between the representation of two distinct regions (registration). Nonrigid registration of 2D and 3D medical images is necessary in order to study the evolution of a pathology in an individual, or to take full advantage of the complementary information coming from multimodality imagery [Maintz & Viergever, 1998; Goshtasby *et al.*, 2003]. Examples of the use of deformable models to perform medical image registration are found in [Moshfeghi, 1991; Moshfeghi *et al.*, 1994; Gueziec & Ayache, 1994; Feldmar & Ayache, 1994; Bookstein, 1989; Hamadeh *et al.*, 1995; Lavallée & Szeliski, 1995; Thirion, 1994]. These techniques primarily consist of constructing highly structured descriptions for matching. This operation is usually carried out by extracting regions

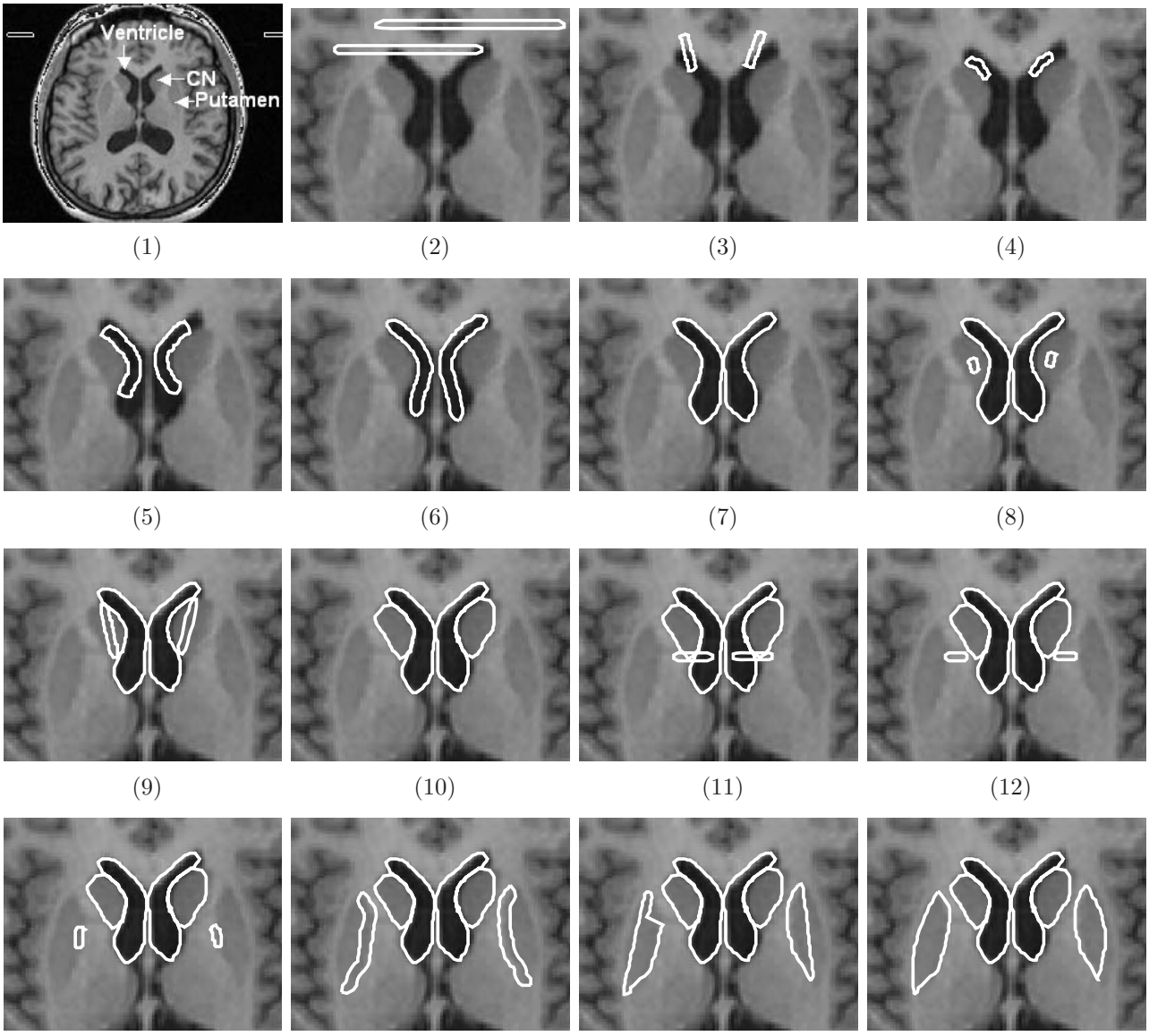

Figure 7: Automatic brain MR image segmentation by multiple deformable organisms (from [McInerney *et al.*, 2002]). The sequence of images illustrates the temporal progression of the segmentation process. Deformable lateral ventricle (1–7), caudate nucleus (8–10), and putamen (11–16) organisms are spawned in succession and progress through a series of behaviors to detect, localize, and segment the corresponding structures in the MR image.

of interest with an edge detection algorithm, followed by the extraction of landmark points or characteristic contours (or curves on extracted boundary surfaces in the case of 3D data). In 3D, these curves usually describe differential structures such as ridges, or topological singularities. An elastic matching algorithm can then be applied between corresponding pairs of curves or contours where the "start" contour is iteratively deformed to the "goal" contour using forces derived from local pattern matches with the goal contour [Moshfeghi, 1991].

An example of matching where the use of explicit prior knowledge has been embedded into deformable models is the automatic extraction and labeling of anatomic structures in the brain from MR images, or the registration of multimodality brain images. The anatomical knowledge is made explicit in the form of a 3D brain atlas. The atlas is modeled as a physical object and is given elastic properties. After an initial global alignment, the atlas deforms and matches itself onto corresponding regions in the brain image volume in response to forces derived from image features. The assumption underlying this approach is that at some representational level, normal brains have the same topological structure and differ only in shape details. The idea of modeling the atlas as an elastic object was originated by Broit [1981], who formulated the matching process as a minimization of a cost function. Subsequently, Bajcsy and Kovacic [1989] implemented a multiresolution version of Broit's system where the deformation of the atlas proceeds step-by-step in a coarse to fine strategy, increasing the local similarity and global coherence. An earlier work with similar objectives, albeit not applied to medical image analysis, was that by Witkin et al. [Witkin *et al.*, 1987], who formulated the general nonrigid registration problem—i.e., that of matching any number of arbitrary-dimensional images or signals—as one of minimizing a nonconvex energy functional combining a controlled-continuity generalized spline deformation energy with normalized cross-correlation and efficiently solved it using an innovative scale-space continuation method. The elastically deformable atlas technique is very promising and consequently has become a very active area of research that is being explored by several groups [Evans *et al.*, 1991; Gee, 1999; Sandor & Leahy, 1995; Christensen *et al.*, 1995; Bookstein, 1991; Bozma & Duncan, 1992; Declerck *et al.*, 1995; McDonald *et al.*, 1994; Delibasis & Undrill, 1994; Subsol *et al.*, 1995; Davatzikos *et al.*, 1996; Snell *et al.*, 1995; Thompson & Toga, 1996-7; Vaillant & Davatzikos, 1997; Wang & Staib, 1998].

The automatic brain image matching problem is extremely challenging and there are many hurdles that must be overcome before the deformable atlas technique can be adopted for clinical use. For example, the technique is sensitive to the initial positioning of the atlas—if the initial rigid alignment is off by too much, then the elastic match may perform poorly. The presence of neighboring features may also cause matching problems—the atlas may warp to an incorrect boundary. Finally, without user interaction, the atlas can have difficulty converging to complicated object boundaries. A proposed solution to these problems is to use image preprocessing in conjunction with the deformable atlas. Sandor and Leahy [1995] use this approach to automatically label regions of the cortical surface that appear in 3D MR images of human brains (Fig. 8). They automatically match a labeled deformable atlas model to preprocessed brain images, where preprocessing consists of 3D edge detection and morphological operations. These filtering operations automatically extract the brain and sulci (deep grooves in the cortical surface) from an MR image and provide a smoothed representation of the brain surface to which their 3D B-spline deformable surface model can rapidly converge.

3.5 Motion Tracking and Analysis

The idea of tracking objects in time-varying images using deformable models was originally proposed in the context of computer vision [Kass *et al.*, 1988; Terzopoulos *et al.*, 1988]. Deformable models have been used to track nonrigid microscopic and macroscopic structures in motion, such as blood cells [Leymarie & Levine, 1993] and neurite growth cones [Gwydir *et al.*, 1994] in cine-microscopy,

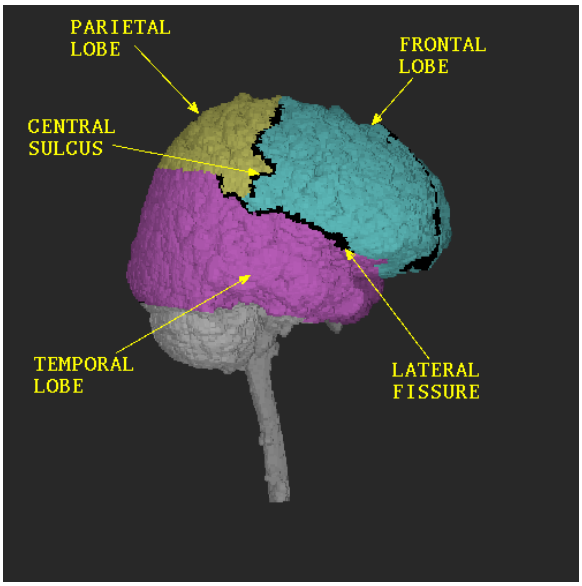

Figure 8: The result of matching a labeled deformable atlas to a morphologically preprocessed MR image of the brain (from [Sandor & Leahy, 1995]).

as well as coronary arteries in cine-angiography [Lengyel *et al.*, 1995]. However, the primary use of deformable models for tracking in medical image analysis is to measure the dynamic behavior of the human heart, especially the left ventricle. Regional characterization of the heart wall motion is necessary to isolate the severity and extent of diseases such as ischemia. Magnetic resonance and other imaging technologies can now provide time varying three dimensional images of the heart with excellent spatial resolution and reasonable temporal resolutions. Deformable models are well suited for this image analysis task.

In the simplest approach, a 2D deformable contour model is used to segment the LV boundary in each slice of an initial image volume. These contours are then used as the initial approximation of the LV boundaries in corresponding slices of the image volume at the next time instant and are then deformed to extract the new set of LV boundaries [Singh *et al.*, 1993; Ueda & Mase, 1992; Ayache *et al.*, 1992; Herlin & Ayache, 1992; Geiger *et al.*, 1995]. This temporal propagation of the deformable contours dramatically decreases the time taken to segment the LV from a sequence of image volumes over a cardiac cycle. Singh *et al.* [1993] report a time of 15 minutes to perform the segmentation, considerably less than the 1.5-2 hours that a human expert takes for manual segmentation. Deformable contour models have also been successfully used to track the LV boundary in noisy echocardiographic image sequences [Jacob *et al.*, 1999; Chalana *et al.*, 1996].

McInerney and Terzopoulos [1995a] have applied the temporal propagation approach in 3D using a 3D dynamic deformable "balloon" model to track the contractile motion of the LV (Fig. 9,10).

In a more involved approach, Amini and Duncan [1992] use bending energy and surface curvature to track and analyze LV motion. For each time instant, two sparse subsets of surface points are created by choosing geometrically significant landmark points, one for the endocardial surface, and the other for the epicardial surface of the LV. Surface patches surrounding these points are then modeled as thin, flexible plates. Making the assumption that each surface patch deforms only slightly and locally within a small time interval, for each sampled point on the first surface they construct a search area on the LV surface in the image volume at the next time instant. The best matched (i.e. minimum bending energy) point within the search window on the second surface is taken to correspond to the point on the first surface. This matching process yields a set of initial

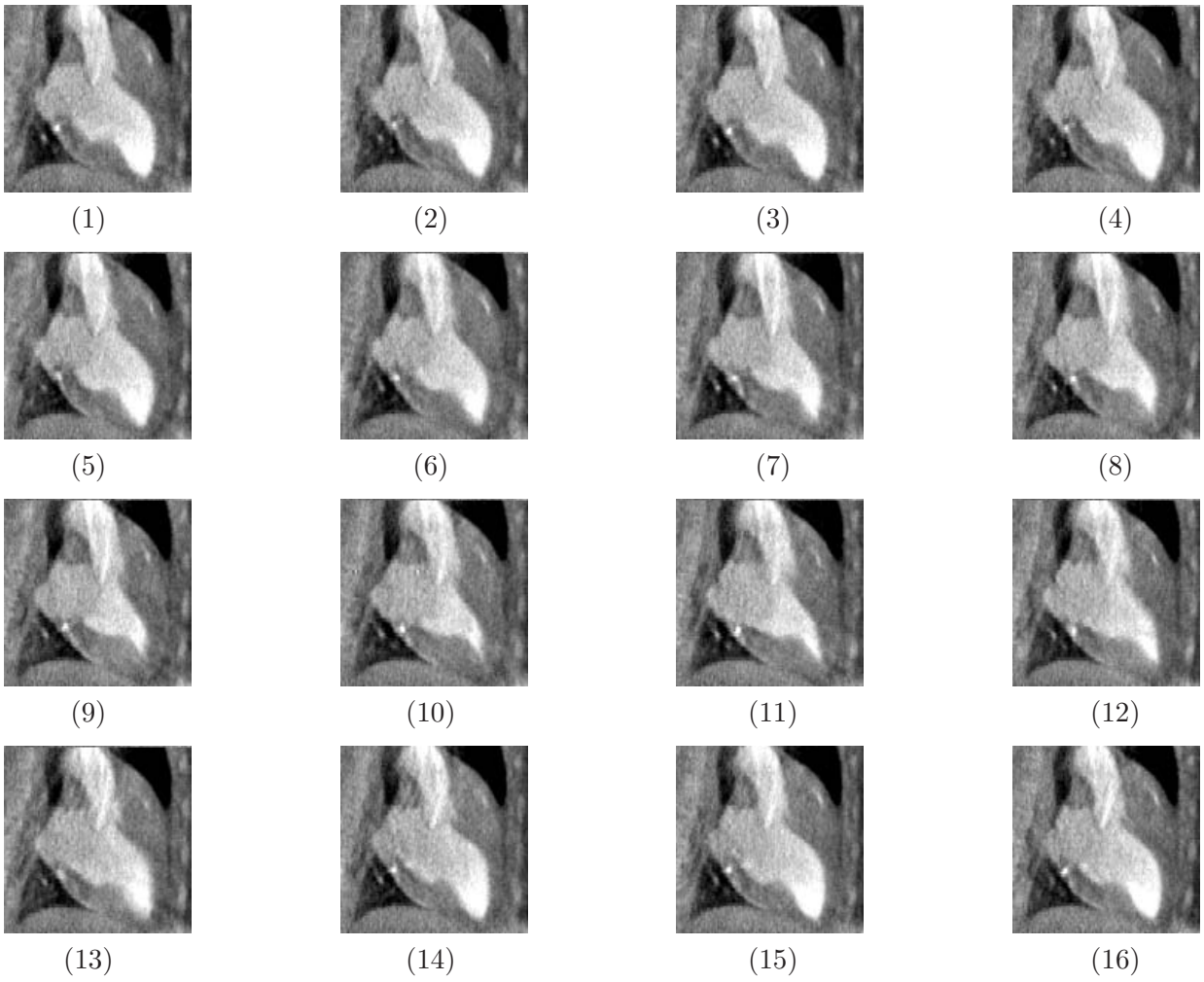

Figure 9: Sagittal slice of successive CT volumes over one cardiac cycle (1–16) showing motion of canine LV (from [McInerney & Terzopoulos, 1995a]).

motion vectors for pairs of LV surfaces derived from a 3D image sequence. A smoothing procedure is then performed using the initial motion vectors to generate a dense motion vector field over the LV surfaces.

Cohen *et al.* [1992a] also employ a bending energy technique in 2D and attempt to improve on this method by adding a term to the bending energy function that tends to preserve the matching of high curvature points. Goldgof *et al.* [Goldgof *et al.*, 1988; Kambhamettu & Goldgof, 1994; Huang & Goldgof, 1993; Mishra *et al.*, 1991] have also been pursuing surface shape matching ideas primarily based on changes in Gaussian curvature and assume a conformal motion model (i.e. motion which preserves angles between curves on a surface but not distances).

An alternative approach is that of Chen *et al.* [1994], who use a hierarchical motion model of the LV constructed by combining a globally deformable superquadric with a locally deformable surface using spherical harmonic shape modeling primitives. Using this model, they estimate the LV motion from angiographic data and produce a hierarchical decomposition that characterizes the LV motion in a coarse-to-fine fashion.

Pentland and Horowitz [1991] and Nastar and Ayache [1996] are also able to produce a coarse-to-

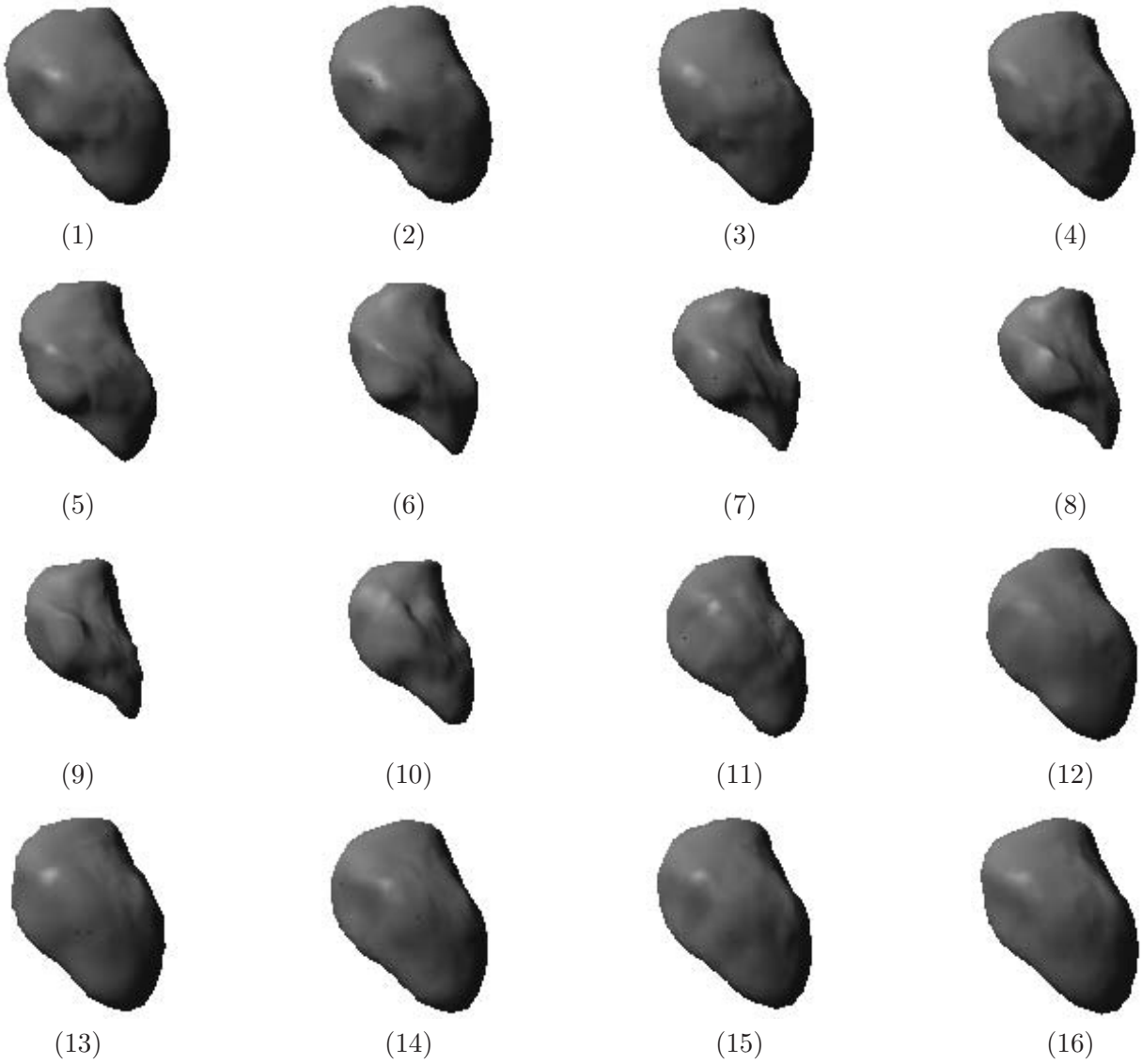

Figure 10: Tracking of the LV motion of canine heart during one cardiac cycle (1–16) using deformable balloon model (from [McInerney & Terzopoulos, 1995a]).

fine characterization of the LV motion. They use dynamic deformable models to track and recover the LV motion and make use of modal analysis, a well-known mechanical engineering technique, to parameterize their models. This parameterization is obtained from the eigenvectors of a finite element formulation of the models. These eigenvectors are often referred to as the "free vibration" modes and variable detail of LV motion representation results from varying the number of modes used.

The heart is a relatively smooth organ and consequently there are few reliable landmark points. The heart also undergoes complex nonrigid motion that includes a twisting (tangential) component as well as the normal component of motion. The motion recovery methods described above are, in general, not able to capture this tangential motion without additional information. Magnetic resonance techniques, based on magnetic tagging [Axel & Dougherty, 1989] have been developed to track material points on the myocardium in a non-invasive way. The temporal correspondence of material points that these techniques provide allow for quantitative measurement of tissue motion and deformation including the twisting component of the LV motion. Several researchers have applied deformable models to image sequences of MR tagged data [Young *et al.*, 1993, 1995; Park *et al.*, 1996; Duncan *et al.*, 1994; Kumar & Goldgof, 1994; Kraitchman *et al.*, 1995; Amini *et al.*, 1998]. For example, Amini *et. al* [1998] and Kumar and Goldgof [1994] use a 2D deformable grid to localize and track SPAMM (Spatial Modulation of Magnetization) tag points on the LV tissue. Park *et al.* [1995; 1996] fit a volumetric physics-based deformable model to MRI-SPAMM data of the LV. The parameters of the model are functions which can capture regional shape variations of the LV such as bending, twisting, and contraction. Based on this model, the authors quantitatively compare normal hearts and hearts with hypertrophic cardiomyopathy.

Another problem with most of the methods described above is that they model the endocardial and epicardial surfaces of the LV separately. In reality the heart is a thick-walled structure. Duncan *et al.* [1994] and Park *et al.* [1995; 1996] develop models which consider the volumetric nature of the heart wall. These models use the shape properties of the endocardial and epicardial surfaces and incorporate mid-wall displacement information of tagged MR images. By constructing 3D finite element models of the LV with nodes in the mid-wall region as well as nodes on the endocardial and epicardial surfaces, more accurate measurements of the LV motion can be obtained. Young and Axel [1992; 1995], and Creswell [1992] have also constructed 3D finite element models from the boundary representations of the endocardial and epicardial surfaces.

4 Discussion

In the previous sections we have surveyed the considerable and still rapidly expanding body of work on deformable models in medical image analysis. The survey has revealed several issues that are relevant to the continued development of the deformable model approach. This section summarizes key issues and indicates some promising research directions.

4.1 Autonomy vs Control

Interactive (semi-automatic) algorithms and fully automatic algorithms represent two alternative approaches to computerized medical image analysis. Certainly automatic interpretation of medical images is a desirable, albeit very difficult, long-term goal, since it can potentially increase the speed, accuracy, consistency, and reproducibility of the analysis. However, the interactive or semi-automatic methodology is likely to remain dominant in practice for some time to come, especially in applications where erroneous interpretations are unacceptable. Consequently, the most immediately successful deformable model based techniques will likely be those that drastically decrease the labor intensiveness of medical image processing tasks through partial automation and significantly

increase their reproducibility, while still allowing for interactive guidance or editing by the medical expert. Although fully automatic techniques based on deformable models will likely not reach their full potential for some time to come, they can be of immediate value in specific application domains such as the segmentation of healthy tissue surrounding a pathology for enhanced visualization.

4.2 Generality vs Specificity

Ideally a deformable model should be capable of representing a broad range of shapes and be useful in a wide array of medical applications. Generality is the basis of deformable model formulations with local shape parameters such as snakes. Alternatively, highly specific, "hand-crafted" or constrained deformable models appear to be useful in applications such as tracking the nonrigid motion of the heart (Section 3.5), automatically matching and labeling structures in the brain from 3D MR images (Section 3.4), or segmenting very noisy images such as echocardiograms. Certainly attempts to completely automate the processing of medical images would require a high degree of application and model specificity. A promising direction for future study appears to be techniques for learning "tailored" models from simple general purpose models. The work of Cootes *et al.* [1994] may be viewed as an example of such a strategy.

4.3 Compactness vs Geometric Coverage vs Topological Flexibility

A geometric model of shape may be evaluated based on the parsimony of its formulation, its representational power, and its topological flexibility. Generally, parameterized models offer the greatest parsimony, free-form (spline) models feature the broadest coverage, and implicit models have the greatest topological flexibility. Deformable models have been developed based on each of these geometric classes. Increasingly, researchers are turning to the development of hybrid deformable models that combine complementary features. For objects with a simple, fixed topology and without significant protrusions, parameterized models coupled with local (spline) and/or global deformations schemes appear to provide a good compactness-descriptiveness tradeoff [Terzopoulos & Metaxas, 1991; Pentland & Horowitz, 1991; Vemuri & Radisavljevic, 1994; Chen *et al.*, 1994]. On the other hand, the segmentation and modeling of complex, multipart objects such as arterial or bronchial "tree" structures, or topologically complex structures such as vertebrae, is a difficult task with these types of models [McInerney & Terzopoulos, 1999]. Polygon based or particle based deformable modeling schemes seem promising in segmenting and reconstructing such structures. Polygon based models may be compacted by removing and "retiling" [Turk, 1992; Gourdon, 1995; Delingette, 1997] polygons in regions of low shape variation, or by replacing a region of polygons with a single, high-order finite element or spline patch [Qin *et al.*, 1998]. A possible research direction is to develop alternative models that blend or combine descriptive primitive elements (rather than simple particles), such as flexible cylinders, into a global structure.

4.4 Curve vs Surface vs Solid Models

The earliest deformable models were curves and surfaces. Anatomic structures in the human body, however, are either solid or thick-walled. To support the expanding role of medical images into tasks such as surgical planning and simulation, and the functional modeling of structures such as bones, muscles, skin, or arterial blood flow, may require volumetric or solid deformable models rather than surface models. For example, the planning of facial reconstructive surgery requires the extraction and reconstruction of the skin, muscles, and bones from 3D images using accurate solid models. It also requires the ability to simulate the movement and interactions of these structures in response to forces, the ability to move, cut and fuse pieces of the model in a realistic fashion, and the ability to stimulate the simulated muscles of the model to predict the effect of the surgery. Several

researchers have begun to explore the use of volumetric or solid deformable models of the human face and head for computer graphics applications [Lee *et al.*, 1995; Essa *et al.*, 1993] and for medical applications [Waters, 1992; Delingette *et al.*, 1994; Pieper *et al.*, 1992; Geiger, 1992; Keeve *et al.*, 1998; Gibson *et al.*, 1998; Wells *et al.*, 1998], particularly reconstructive surgery simulation, and there is much room for further research. Researchers have also begun to use volumetric deformable models to more accurately track and analyze LV motion [Young & Axel, 1992; Creswell *et al.*, 1992; Duncan *et al.*, 1994; Park *et al.*, 1996].

4.5 Accuracy and Quantitative Power

Ideally it should be possible to measure and control the accuracy of a deformable model. The most common accuracy control mechanisms are the global or local subdivision of model basis functions [Miller *et al.*, 1991], or the repositioning of model points to increase their density in regions of the data exhibiting rapid shape variations [Vasilescu & Terzopoulos, 1992]. Other mechanisms that warrant further research are the local control and adaptation of model continuity, parameter evolution (including the rate and scheduling of the evolution), and the automation of all accuracy control mechanisms. The parametric formulation of a deformable model should not only yield an accurate description of the object, but it should also provide quantitative information about the object in an intuitive, convenient form. That is, the model parameters should be useful for operations such as measuring, matching, modification, rendering, and higher-level analysis or geometric reasoning. This "parameter descriptiveness" criterion may be achieved in a postprocessing step by adapting or optimizing the parameterization to more efficiently or more descriptively match the data. However, it is preferable to incorporate the descriptive parameterization directly into the model formulation. An example of this strategy is the deformable model of Park *et al.* [1996].

4.6 Robustness

Ideally, a deformable model should be insensitive to initial conditions and noisy data. Deformable models are able to exploit multiple image attributes and high level or global information to increase the robustness of shape recovery. For example, many snakes models now incorporate region based image features as well as the traditional edge based features (Section 3.1). Strategies worthy of further research include the incorporation of shape constraints into the deformable model that are derived from low level image processing operations such as thinning, medial axis transforms [Fritsch *et al.*, 1997], or mathematical morphology. A classical approach to improve the robustness of model fitting is the use of multiscale image preprocessing techniques [Kass *et al.*, 1988; Terzopoulos *et al.*, 1988], perhaps coupled with a multiresolution deformable model [Bajcsy & Kovacic, 1989]. A multiresolution technique that merits further research in the context of deformable models, is the use of wavelet bases [Strang & Nguyen, 1996] for deformations [Vemuri *et al.*, 1993; Vemuri & Radisavljevic, 1994]. A deformable model should be able to easily incorporate added constraints and any other *a priori* anatomic knowledge of object shape and motion. Section 3.3 reviewed several of the most promising techniques to incorporate *a priori* knowledge. For example, for LV motion tracking, a promising research direction is the incorporation of biomechanical properties of the heart and the inclusion of the temporal periodic characteristics of the heart motion. Future directions include modeling schemes that incorporate reasoning and recognition mechanisms using techniques from artificial intelligence, such as rule-based systems or neural networks, and techniques from artificial life [McInerney *et al.*, 2002].

4.7 Lagrangian vs Eulerian Deformable Models

An alternative to the Lagrangian formulation of deformable models upon which this survey has focused, is the Eulerian formulation. The latter leads to so called *level set methods*, which have attracted much attention in the medical image analysis literature. Covering the now voluminous literature is beyond the scope of this survey, but we point the reader to the recent volume by Osher and Paragios [2003] and recent survey articles [Suri *et al.*, 2002; Tsai & Osher, 2003; Cremers *et al.*, 2007] for relevant background material and references. The important point is that the two approaches are complementary in precisely the same sense that Lagrangian solid models complement Eulerian fluid models in continuum mechanics and that parametric and implicit geometric models complement one another in computer-aided geometric design. The substantial medical image analysis literature on Lagrangian and Eulerian deformable models is a testament to the fact that each approach is useful in particular applications.

The initial motivation for the Eulerian formulation of deformable models was to introduce topological flexibility into the model-based image segmentation problem through the adaptation of the Osher-Sethian level set evolution technique [Caselles *et al.*, 1993; Malladi *et al.*, 1995; Whitaker, 1994; Caselles *et al.*, 1995; Sapiro *et al.*, 1995]. Formulated as evolving contours (surfaces in 3D) or "fronts" which define the level set of some higher-dimensional (hyper-) surface over the image domain, the main feature of this approach is that topological changes are handled naturally, since the level set need not be simply connected; the higher-dimensional surface remains a simple function even as the level set changes topology. While the level set technique is an attractive mathematical framework, partial differential equations governing curvature-dependent front evolution, implicit formulations are generally not as convenient as the explicit, parametric formulations when it comes to incorporating additional control mechanisms including internal deformation energies and external interactive guidance by expert users. Furthermore, the higher-dimensional implicit surface formulation makes it difficult to impose arbitrary geometric or topological constraints on the level set indirectly through the higher dimensional representation. Therefore, the implicit formulation may potentially limit the ease of use, efficiency and degree of automation achievable in the segmentation task.

Among newer approaches that address these difficulties are T-snakes and T-surfaces [McInerney & Terzopoulos, 2000, 1999], which can be viewed as hybrid models that combine aspects of the Lagrangian and Eulerian approaches (with the ACID introducing aspects of the latter to induce topological flexibility). A recent, purely Lagrangian approach that maintains the advantages of level set methods while avoiding their drawbacks is the Delaunay Deformable Models [Pons & Boissonnat, 2007]. This reference provides additional discussion of the shortcomings of the level set method and cites several other recent alternatives to the T-snakes approach.

5 Conclusion

The increasingly important role of medical imaging in the diagnosis and treatment of disease has opened an array of challenging problems centered on the computation of accurate geometric models of anatomic structures from medical images. Deformable models offer an attractive approach to tackling such problems, because these models are able to represent the complex shapes and broad shape variability of anatomical structures. Deformable models overcome many of the limitations of traditional low-level image processing techniques, by providing compact and analytical representations of object shape, by incorporating anatomic knowledge, and by providing interactive capabilities. The continued development and refinement of these models should remain an important area of research into the foreseeable future.

Acknowledgements

We acknowledge our collaborators who have assisted in the development of the deformable model based approach to medical image analysis, especially Ghassan Hamarneh and Jianming Liang. We would like to thank Stephanie Sandor and Richard Leahy of the USC Signal and Image Processing Institute for the deformable brain atlas figure, as well as the following individuals for providing citation information that improved the completeness of the bibliography: Amir Amini, Nicholas Ayache, Ingrid Carlbom, Chang Wen Chen, James Duncan, Dmitry Goldgof, Thomas Huang, Stephane Lavallee, Francois Leitner, Gerard Medioni, Dimitris Metaxas, Alex Pentland, Stan Sclaroff, Ajit Singh, Richard Szeliski, Baba Vemuri, Alistair Young, and Alan Yuille. The preparation of the first version of this survey [McInerney & Terzopoulos, 1996] was made possible by the financial support of the Information Technologies Research Center of Ontario.

References

Amini, A., Chen, Y., Curwen, R., Mani, V., & Sun, J. 1998. Coupled B-snake grids and constrained thin-plate splines for analysis of 2D tissue deformation from tagged MRI. *Ieee trans. on medical imaging*, **17**(3), 344–356. 20

Amini, A.A., & Duncan, J.S. 1992. Bending and stretching models for LV wall motion analysis from curves and surfaces. *Image and vision computing*, **10**(6), 418–430. 17

Amini, A.A., Weymouth, T.E., & Jain, R.C. 1990. Using dynamic programming for solving variational problems in vision. *Ieee trans. on pattern analysis and machine intelligence*, **12**(9), 855–867. 9

Axel, L., & Dougherty, L. 1989. Heart wall motion: Improved method of spatial modulation of magnetization for MR imaging. *Radiology*, **172**, 349–350. 20

Ayache, N. 1995a. Medical computer vision, virtual reality and robotics. *Image and vision computing*, **13**(4), 295–313. 3

Ayache, N. (ed). 1995b. *Proc. first international conf. on computer vision, virtual reality and robotics in medicine (cvrmed'95), nice, france, april*. Lectures Notes in Computer Science, vol. 905. Berlin, Germany: Springer-Verlag. 3, 26, 28

Ayache, N., Cohen, I., & Herlin, I.L. 1992. Medical image tracking. *Chap. 17, pages 285–302 of:* Blake, A., & Yuille, A. (eds), *Active vision*. Cambridge, MA: MIT Press. 17

Bajcsy, R., & Kovacic, S. 1989. Multiresolution elastic matching. *Computer vision, graphics, and image processing*, **46**, 1–21. 16, 22

Ballard, D., & Brown, C. 1982. *Computer vision*. Englewood Cliffs, NJ: Prentice-Hall. 7

Bardinet, E., Cohen, L.D., & Ayache, N. 1996. Tracking and motion analysis of the left ventricle with deformable superquadrics. *Medical image analysis*, **1**(2), 129–149. 13

Barrett, W.A., & Mortensen, E.N. 1996-7. Interactive live-wire boundary extraction. *Medical image analysis*, **1**(4), 331–341. 10

Berger, M.O. 1990. Snake growing. *Pages 570–572 of:* Faugeras, O. (ed), *Proc. first european conf. on computer vision (eccv'90), antibes, france, april*. Lectures Notes in Computer Science. Springer-Verlag. 9

Bizais, Y., Barillot, C., & Paola, R. Di (eds). 1995. *Information processing in medical imaging: Proc. 14th int. conf. (ipmi'95), ile de berder, france, june.* Computational Imaging and Vision, vol. 3. Dordrecht, The Netherlands: Kluwer Academic. 3, 25, 30, 32

Bookstein, F.L. 1989. Principal warps: Thin-plate splines and the decomposition of deformations. *Ieee trans. on pattern analysis and machine intelligence*, **11**(6), 567–585. 14

Bookstein, F.L. 1991. Thin-plate splines and the atlas problem for biomedical images. *Pages 326–342 of:* Barret, H.H., & Gmitro, A.F. (eds), *Information processing in medical imaging: Proc. 12th int. conf. (ipmi'91), wye, uk, july.* Lectures Notes in Computer Science. Springer-Verlag. 16

Bozma, I., & Duncan, J.S. 1992. A modular system for image analysis using a game theoretic framework. *Image and vision computing*, **10**(6), 431–443. 16

Broit, C. 1981. *Optimal registration of deformed images.* Ph.D. thesis, Computer and Information Science Dept., University of Pennsylvania, Philadelphia, PA. 16

Carlbom, I., Terzopoulos, D., & Harris, K. 1994. Computer-assisted registration, segmentation, and 3D reconstruction from images of neuronal tissue sections. *Ieee trans. on medical imaging*, **13**(2), 351–362. 5, 9

Caselles, V., Catte, F., Coll, T., & Dibos, F. 1993. A geometric model for active contours in image processing. *Numerische mathematik*, **66**, 1–31. 23

Caselles, V., Kimmel, R., & Sapiro, G. 1995. Geodesic active contours. *Pages 694–699 of: Proc. fifth international conf. on computer vision (iccv'95), cambridge, ma, june.* 10, 23

Caselles, V., Kimmel, R., & Sapiro, G. 1997. Minimal surfaces based object segmentation. *Ieee trans. on pattern analysis and machine intelligence*, **19**(4). 10, 12

Chakraborty, A., & Duncan, J.S. 1999. Game theoretic integration for image segmentation. *Ieee trans. on pattern analysis and machine intelligence*, **21**(1). 10

Chalana, V., Linker, D.T., Haynor, D.R., & Kim, Y. 1996. A multiple active contour model for cardiac boundary detection on echocardiographic sequences. *Ieee trans. on medical imaging*, **15**, 290–298. 17

Chang, L.W., Chen, H.W., & Ho, J.R. 1991. Reconstruction of 3D medical images: A nonlinear interpolation technique for reconstruction of 3D medical images. *Computer vision, graphics, and image processing*, **53**(4), 382–391. 9

Chen, C.W., Huang, T.S., & Arrott, M. 1994. Modeling, analysis and visualization of left ventricle shape and motion by hierarchical decomposition. *Ieee trans. on pattern analysis and machine intelligence*, **16**(April), 342–356. 13, 18, 21

Christensen, G., Rabbitt, R.D., Miller, M.I., Joshi, S.C., Grenander, U., Coogan, T.A., & van Essen, D.C. 1995. Topological properties of smooth anatomic maps. *In:* [Bizais *et al.*, 1995]. 16

Cohen, I., Ayache, N., & Sulger, P. 1992a. Tracking points on deformable objects using curvature information. *Pages 458–466 of:* Sandini, G. (ed), *Proc. second european conf. on computer vision (eccv'92), santa margherita ligure, italy, may.* Lectures Notes in Computer Science. Springer-Verlag. 18

Cohen, I., Cohen, L.D., & Ayache, N. 1992b. Using deformable surfaces to segment 3D images and infer differential structures. *Cvgip: Image understanding*, **56**(2), 242–263. 11

Cohen, L.D. 1991. On active contour models and balloons. *Cvgip: Image understanding*, **53**(2), 211–218. 9

Cohen, L.D., & Cohen, I. 1993. Finite element methods for active contour models and balloons for 2D and 3D images. *Ieee trans. on pattern analysis and machine intelligence*, **15**(11), 1131–1147. 9, 11

Cootes, T., Hill, A., Taylor, C., & Haslam, J. 1994. The use of active shape models for locating structures in medical images. *Image and vision computing*, **12**(6), 355–366. 14, 21

Cremers, D., Rousson, Mikael, & Deriche, Rachid. 2007. A review of statistical approaches to level set segmentation: Integrating color, texture, motion and shape. *International journal of computer vision*, **72**(2), 195–215. 23

Creswell, L.L., Wyers, S.G., Pirolo, J.S., Perman, W.H., Vannier, M.W., & Pasque, M.K. 1992. Mathematical modelling of the heart using magnetic resonance imaging. *Ieee trans. on medical imaging*, **11**(4), 581–589. 20, 22

Davatzikos, C., & Bryan, R.N. 1995. Using a deformable surface model to obtain a mathematical representation of the cortex. *Pages 212–217 of: International symp. on computer vision, coral gables, fl, november, 1995*. 12

Davatzikos, C.A., & Prince, J.L. 1995. An active contour model for mapping the cortex. *Ieee trans. on medical imaging*, **14**(1), 65–80. 9

Davatzikos, C.A., Prince, J.L., & Bryan, R.N. 1996. Image registration based on boundary mapping. *Ieee trans. on medical imaging*, **15**(1), 112–115. 16

Declerck, J., Subsol, G., Thirion, J.P., & Ayache, N. 1995. Automatic retrieval of anatomic structures in 3D medical images. *In:* [Ayache, 1995b]. 16

Delibasis, K., & Undrill, P.E. 1994. Anatomical object recognition using deformable geometric models. *Image and vision computing*, **12**(7), 423–433. 16

Delibasis, K., Undrill, P.E., & Cameron, G.G. 1997. Designing Fourier descriptor-based geometric models for object interpretation in medical images using genetic algorithms. *Computer vision and image understanding*, **66**(3), 286–300. 12

Delingette, H. 1997. Decimation of iso-surfaces with deformable models. *In:* [Troccaz *et al.*, 1997]. 21

Delingette, H., Hebert, M., & Ikeuchi, K. 1992. Shape representation and image segmentation using deformable surfaces. *Image and vision computing*, **10**(3), 132–144. 12

Delingette, H., Subsol, G., Cotin, S., & Pignon, J. 1994. Virtual reality and craniofacial surgery simulation. *In:* [Robb, 1994]. 22

Duncan, J., & Gindi, G. (eds). 1997. *Information processing in medical imaging: Proc. 15th int. conf. (ipmi'97), poultney, vermont, usa, june*. Lecture Notes in Computer Science, vol. 1230. Berlin, Germany: Springer. 3, 27, 29, 34

Duncan, J., Shi, P., Amini, A., Constable, R., Staib, L., Dione, D., Shi, Q., Heller, E., Singer, M., Chakraborty, A., Robinson, G., Gore, J., & Sinusas, A. 1994. Towards reliable, noninvasive measurement of myocardial function from 4D images. *Pages 149–161 of: Medical imaging 1994: Physiology and function from multidimensional medical images.* SPIE Proc., vol. 2168. Bellingham, WA: SPIE. 20, 22

Duncan, J.S., & Ayache, N. 2000. Medical image analysis: Progress over two decades and the challenges ahead. *Ieee transactions on pattern analysis and machine intelligence*, **22**(1), 85–106. 3

Duta, N., & Sonka, M. 1998. Segmentation and interpretation of MR brain images: An improved active shape model. *Ieee trans. on medical imaging*, **17**(6), 1049–1062. 14

Essa, I., Sclaroff, S., & Pentland, A.P. 1993. Physically-based modeling for graphics and vision. *Pages 160–196 of:* Martin, R. (ed), *Directions in geometric computing.* Information Geometers, U.K. 22

Evans, A.C., Dai, W., Collins, L., Neelin, P., & Marrett, S. 1991. Warping of a computerized 3D atlas to match brain image volumes for quantitative neuroanatomical and functional analysis. *Pages 236–246 of: Medical imaging v: Image processing.* SPIE Proc., vol. 1445. 16

Falcão, A., Udupa, J., Samarasekera, S., Sharma, S., Hirsch, B.E., & de A. Lotufo, R. 1998. User-steered image segmentation paradigms: Live wire and live lane. *Graphical models and image processing*, **60**(4), 233–60. 10

Farin, G. 1993. *Curves and surfaces for cagd.* New York: Academic Press. 7

Feldmar, J., & Ayache, N. 1994. Locally affine registration of free-form surfaces. *Pages 496–501 of: Proc. conf. computer vision and pattern recognition (cvpr'94), seattle, wa, june.* 14

Fischler, M., & Elschlager, R. 1973. The representation and matching of pictorial structures. *Ieee trans. on computers*, **22**(1), 67–92. 4, 13

Fritsch, D., Pizer, S.M., Yu, L., Johnson, V., & Chaney, E. 1997. Segmentation of medical image objects using deformable shape loci. *In:* [Duncan & Gindi, 1997]. 22

Gauch, J.M., Pien, H.H., & Shah, J. 1994. Hybrid boundary-based and region-based deformable models for biomedical image segmentation. *Pages 72–83 of: Mathematical methods in medical imaging iii.* SPIE Proc., vol. 2299. San Diego, CA: SPIE. 10

Gee, J.C. 1999. On matching brain volumes. *Pattern recognition*, **32**, 99–111. 13, 16

Geiger, B. 1992 (October). Three dimensional simulation of delivery for cephalopelvic disproportion. *Pages 146–152 of: First international workshop on mechatronics in medicine and surgery, costa del sol, spain, october, 1992.* 22

Geiger, D., Gupta, A., Costa, L.A., & Vlontzos, J. 1995. Dynamic programming for detecting, tracking and matching deformable contours. *Ieee trans. on pattern analysis and machine intelligence*, **17**(3), 294–302. 17

Gibson, S, Fyock, C, Grimson, E, Kanade, T, Kikinis, R, Lauer, H, McKenzie, N, Mor, A, Nakajima, S, Ohkami, H, Osborne, R, Samosky, J, & Sawada, A. 1998. Volumetric object modeling for surgical simulation. *Medical image analysis*, **2**(2), 121–132. 22

Goldgof, D.B., Lee, H., & Huang, T.S. 1988. Motion analysis of nonrigid surfaces. *Pages 375–380 of: Proc. conf. computer vision and pattern recognition (cvpr'88), ann arbor, mi, june.* 18

Goshtasby, A., Staib, L., Studholme, C., & Terzopoulos, D. 2003. Nonrigid image registration. *Computer vision and image understanding*, **89**(2/3), 109–113. Special Issue on "Nonrigid Image Registration". 14

Gourdon, A. 1995. Simplification of irregular surface meshes in 3D medical images. *In:* [Ayache, 1995b]. 21

Grzeszczuk, R.P., & Levin, D.N. 1997. Brownian strings: Segmenting images with stochastically deformable contours. *Ieee trans. on pattern analysis and machine intelligence*, **19**(10). 10

Gueziec, A., & Ayache, N. 1994. Smoothing and matching of 3D space curves. *International journal of computer vision*, **12**(1), 79–104. 14

Gunn, S.R., & Nixon, M.S. 1997. A robust snake implementation; a dual active contour. *Ieee trans. on pattern analysis and machine intelligence*, **19**(1). 10

Gupta, A., O'Donnell, T., & Singh, A. 1994 (September). Segmentation and tracking of cine cardiac MR and CT images using a 3-D deformable model. *Pages 661–664 of: Proc. ieee conf. on computers in cardiology.* 9

Gwydir, S.H., Buettner, H.M., & Dunn, S.M. 1994. Non-rigid motion analysis and feature labelling of the growth cone. *Pages 80–87 of: Ieee workshop on biomedical image analysis.* Seattle, WA: IEEE Computer Society Press. 16

Hamadeh, A., Lavallee, S., Szeliski, R., Cinquin, P., & Peria, O. 1995. Anatomy-based registration for computer-integrated surgery. *In:* [Ayache, 1995b]. 14

Hamarneh, G., McInerney, T., & Terzopoulos, D. 2001. Deformable organisms for automatic medical image analysis. *Pages 66–75 of: Proceedings of the third international conference on medical image computing and computer assisted interventions (MICCAI01), utrecht, the netherlands.* Berlin, Germany: Springer. 14

Herlin, I.L., & Ayache, N. 1992. Features extraction and analysis methods for sequences of ultrasound images. *Image and vision computing*, **10**(10), 673–682. 17

Herlin, I.L., Nguyen, C., & Graffigne, C. 1992. A deformable region model using stochastic processes applied to echocardiographic images. *Pages 534–539 of: Proc. conf. computer vision and pattern recognition (cvpr'92), urbana, il, june.* 10

Hill, A., Thornham, A., & Taylor, C.J. 1993. Model-based interpretation of 3D medical images. *Pages 339–348 of: Proc. 4th british machine vision conf. (bmvc'93), surrey, uk, september.* BMVA Press. 14

Höhne, K.H., & Kikinis, R. (eds). 1996. *Proc. fourth conf. on visualization in biomedical computing (vbc'96), hamburg, germany, september.* Lecture Notes in Computer Science, vol. 1131. Berlin, Germany: Springer. 3

Huang, W.C., & Goldgof, D.B. 1993. Adaptive-size meshes for rigid and nonrigid shape analysis and synthesis. *Ieee trans. on pattern analysis and machine intelligence*, **15**(3). 18

Ivins, J., & Porrill, J. 1994. Statistical snakes: Active region models. *Pages 377–386 of: Proc. 5th british machine vision conf. (bmvc'94)*. BMVA Press. 10

Jacob, G., Noble, J.A., Mulet-Parada, M., & Blake, A. 1999. Evaluating a robust contour tracker on echocardiographic sequences. *Medical image analysis*, **3**(1), 63–75. 17

Jones, T., & Metaxas, D. 1997. Automated 3D segmentation using deformable models and fuzzy affinity. *In:* [Duncan & Gindi, 1997]. 10

Kambhamettu, C., & Goldgof, D.B. 1994. Point correspondence recovery in nonrigid motion. *Cvgip: Image understanding*, **60**(1), 26–43. 18

Kass, M., Witkin, A., & Terzopoulos, D. 1988. Snakes: Active contour models. *International journal of computer vision*, **1**(4), 321–331. 4, 9, 16, 22

Keeve, E., Girod, S., Kikinis, R., & Girod, B. 1998. Deformable modeling of facial tissue for craniofacial surgery simulation. *Computer aided surgery*, **3**(5), 228–238. 22

Kraitchman, D.L., Young, A.A., Chang, C.N., & Axel, L. 1995. Semi-automatic tracking of myocardial motion in MR tagged images. *Ieee trans. on medical imaging*, **14**(3), 422–432. 20

Kumar, S., & Goldgof, D. 1994. Automatic tracking of SPAMM grid and the estimation of deformation parameters from cardiac MR images. *Ieee trans. on medical imaging*, **13**(1), 122–132. 20

Lachaud, J.-O., & Montanvert, A. 1999. Deformable meshes with automated topology changes for coarse-to-fine 3D surface extraction. *Medical image analysis*, **3**(2), 187–207. 10

Lavallée, S., & Szeliski, R. 1995. Recovering the position and orientation of free-form objects from image contours using 3D distance maps. *Ieee trans. on pattern analysis and machine intelligence*, **17**(4), 378–390. 14

Lee, Y., Terzopoulos, D., & Waters, K. 1995. Realistic modeling for facial animation. *Pages 55–62 of: Proc. acm siggraph'95, in computer graphics proc., annual conf. series*. Los Angeles, CA: ACM SIGGRAPH. 22

Leitner, F., & Cinquin, P. 1991. Complex topology 3D objects segmentation. *Pages 16–26 of: Model-based vision development and tools*. SPIE Proc., vol. 1609. Bellingham, WA: SPIE. 10

Leitner, F., & Cinquin, P. 1993. From splines and snakes to Snakes Splines. *Pages 264–281 of:* Laugier, C. (ed), *Geometric reasoning: From perception to action*. Lectures Notes in Computer Science, vol. 708. Springer-Verlag. 9

Lengyel, J., Greenberg, D.P., & Popp, R. 1995 (August). Time-dependent three-dimensional intravascular ultrasound. *Pages 457–464 of: Proc. acm siggraph'95 conf., in computer graphics proc., annual conf. series*. 17

Leymarie, F., & Levine, M. 1993. Tracking deformable objects in the plane using an active contour model. *Ieee trans. on pattern analysis and machine intelligence*, **15**(6), 635–646. 16

Liang, J., McInerney, T., & Terzopoulos, D. 1999. Interactive medical image segmentation with united snakes. *Pages 116–127 of: Proceedings of the second international conference on medical image computing and computer assisted interventions (MICCAI99)*. Lectures Notes in Computer Science, vol. 1679. Berlin, Germany: Springer-Verlag. 10

Liang, J., McInerney, T., & Terzopoulos, D. 2006. United snakes. *Medical image analysis*, **10**(2), 215–233. 10

Lin, W.C., & Chen, S.Y. 1989. A new surface interpolation technique for reconstructing 3D objects from serial cross-sections. *Computer vision, graphics, and image processing*, **48**(Oct.), 124–143. 9

Lipson, P., Yuille, A.L., O'Keefe, D., Cavanaugh, J., Taaffe, J., & Rosenthal, D. 1990. Deformable templates for feature extraction from medical images. *Pages 477–484 of:* Faugeras, O. (ed), *Proc. first european conf. on computer vision (eccv'90), antibes, france, april*. Lectures Notes in Computer Science. Springer-Verlag. 13

Lobregt, S., & Viergever, M.A. 1995. A discrete dynamic contour model. *Ieee trans. on medical imaging*, **14**(1), 12–24. 9

Lötjönen, J., Reissman, P-J., Magnin, I.E., & Katila, T. 1999. Model extraction from magnetic resonance volume data using the deformable pyramid. *Medical image analysis*, **3**(4), 387–406. 13

Maintz, B.A, & Viergever, M.A. 1998. A survey of medical image registration. *Medical image analysis*, **2**(1), 1–36. 14

Malladi, R., Sethian, J., & Vemuri, B.C. 1995. Shape modeling with front propagation: A level set approach. *Ieee trans. on pattern analysis and machine intelligence*, **17**(2), 158–175. 10, 23

Malladi, R., Kimmel, R., Adalsteinsson, D., Sapiro, G., Caselles, V., & Sethian, J.A. 1996 (June). A geometric approach to segmentation and analysis of 3D medical images. *Pages 244–252 of: Ieee workshop on mathematical methods in biomedical image analysis*. 10

Mangin, J.F., Tupin, F., Frouin, V., Bloch, I., Rougetet, R., Regis, J., & Lopez-Krahe, J. 1995. Deformable topological models for segmentation of 3D medical images. *In:* [Bizais *et al.*, 1995]. 10

McDonald, D., Avis, D., & Evans, A. 1994. Multiple surface identification and matching in magnetic resonance images. *In:* [Robb, 1994]. 16

McInerney, T., & Kikinis, R. 1998. An object-based volumetric deformable atlas for the improved localization of neuroanatomy in MR images. *In:* [Wells *et al.*, 1998]. 13

McInerney, T., & Terzopoulos, D. 1995a. A dynamic finite element surface model for segmentation and tracking in multidimensional medical images with application to cardiac 4D image analysis. *Computerized medical imaging and graphics*, **19**(1), 69–83. 6, 9, 11, 17, 18, 19

McInerney, T., & Terzopoulos, D. 1995b. Topologically adaptable snakes. *Pages 840–845 of: Proc. fifth international conf. on computer vision (iccv'95), cambridge, ma, june*. 10

McInerney, T., & Terzopoulos, D. 1996. Deformable models in medical image analysis: A survey. *Medical image analysis*, **1**(2), 91–108. 3, 24

McInerney, T., & Terzopoulos, D. 1997. Medical image segmentation using topologically adaptable surfaces. *In:* [Troccaz *et al.*, 1997]. 12

McInerney, T., & Terzopoulos, D. 1999. Topology adaptive deformable surfaces for medical image volume segmentation. *IEEE transactions on medical imaging*, **18**(10), 840–850. 12, 21, 23

McInerney, T., & Terzopoulos, D. 2000. T-snakes: Topology adaptive snakes. *Medical image analysis*, **4**(2), 73–91. 9, 10, 12, 23

McInerney, T., Hamarneh, G., Shenton, M., & Terzopoulos, D. 2002. Deformable organisms for automatic medical image analysis. *Medical image analysis*, **6**(3), 251–266. 14, 15, 22

McIntosh, C., & Hamarneh, G. 2006a. I-DO: A deformable organisms framework for ITK. *Insight journal*, 1–14. Special Issue on "MICCAI 2006 Open Science Workshop". 14

McIntosh, C., & Hamarneh, G. 2006b. Vessel crawlers: 3D physically-based deformable organisms for vasculature segmentation and analysis. *Pages 1084–1091 of: Proceedings of the ieee conference on computer vision and pattern recognition (cvpr'06)*. 14

Metaxas, D., & Terzopoulos, D. 1993. Shape and nonrigid motion estimation through physics-based synthesis. *Ieee trans. on pattern analysis and machine intelligence*, **15**(6), 580–591. 13

Miller, J.V., Breen, D.E., Lorensen, W.E., O'Bara, R.M., & Wozny, M.J. 1991 (July). Geometrically deformed models: A method for extracting closed geometric models from volume data. *Pages 217–226 of: Computer graphics (proc. acm siggraph'91 conf.)*, vol. 25(4). 11, 22

Mishra, S.K., Goldgof, D.B., & Huang, T.S. 1991. Non-rigid motion analysis and epicardial deformation estimation from angiography data. *Pages 331–336 of: Proc. conf. computer vision and pattern recognition (cvpr'91), maui, hi, june*. 18

Montagnat, J., & Delingette, H. 1997. Volumetric medical image segmentation using shape constrained deformable models. *In:* [Troccaz *et al.*, 1997]. 13

Moshfeghi, M. 1991. Elastic matching of multimodality medical images. *Cvgip: Graphical models and image processing*, **53**, 271–282. 14, 16

Moshfeghi, M., Ranganath, S., & Nawyn, K. 1994. Three-dimensional elastic matching of volumes. *Ieee trans. on image processing*, **3**, 128–138. 14

Nastar, C., & Ayache, N. 1996. Frequency-based nonrigid motion analysis: Application to four dimensional medical images. *Ieee trans. on pattern analysis and machine intelligence*, **18**(11). 12, 18

Neuenschwander, W., Fua, P., Székely, G., & Kübler, O. 1997. Velcro surfaces: Fast initialization of deformable models. *Computer vision and image understanding*, **65**(2), 237–245. 12

Niessen, W., ter Haar Romeny, B.M., & Viergever, M.A. 1998. Geodesic deformable models for medical image analysis. *Ieee trans. on medical imaging*, **17**(4), 634–641. 10

Osher, S., & Paragios, N. (eds). 2003. *Geometric level set methods in imaging, vision, and graphics*. New York: Springer-Verlag. 23

Park, J., Metaxas, D., & Axel, L. 1995. Volumetric deformable models with parameter functions: A new approach to the 3D motion analysis of the LV from MRI-SPAMM. *Pages 700–705 of: Proc. fifth international conf. on computer vision (iccv'95), cambridge, ma, june*. 20

Park, J., Metaxas, D., & Axel, L. 1996. Analysis of left ventricular wall motion based on volumetric deformable models and MRI-SPAMM. *Medical image analysis*, **1**(1). 20, 22

Paulus, D., Wolf, M., Meller, S., & Nieman, H. 1999. Three-dimensional computer vision for tooth restoration. *Medical image analysis*, **3**(1), 1–19. 9

Pentland, A., & Horowitz, B. 1991. Recovery of nonrigid motion and structure. *Ieee trans. on pattern analysis and machine intelligence*, **13**(7), 730–742. 13, 18, 21

Pentland, A., & Sclaroff, S. 1991. Closed-form solutions for physically based shape modelling and recognition. *Ieee trans. on pattern analysis and machine intelligence*, **13**(7), 715–729. 12

Pieper, S., Rosen, J., & Zeltzer, D. 1992. Interactive graphics for plastic surgery: A task-level analysis and implementation. *Pages 127–134 of: Proc. acm 1992 symposium on interactive 3D graphics*. 22

Pons, J.-P., & Boissonnat, J.-D. 2007 (June). Delaunay deformable models: Topology-adaptive meshes based on the restricted delaunay triangulation. *Pages 1–8 of: Proceedings of the ieee conference on computer vision and pattern recognition (cvpr'07)*. 23

Poon, C. S., Braun, M., Fahrig, R., Ginige, A., & Dorrell, A. 1994. Segmentation of medical images using an active contour model incorporating region-based images features. *In:* [Robb, 1994]. 10

Press, W.H., Teukolsky, S.A., Vetterling, W.T., & Flannery, B.P. 1992. *Numerical recipes in c*. Cambridge University Press. 7

Qin, H., Mandal, C., & Vemuri, B.C. 1998. Dynamic Catmull-Clark subdivision surfaces. *Ieee transactions on visulaization and computer graphics*, **4**(3). 21

Robb, R.A. (ed). 1994. *Proc. third conf. on visualization in biomedical computing (vbc'94), rochester, mn, october*. SPIE Proc., vol. 2359. Bellingham, WA: SPIE. 3, 26, 30, 32, 35

Rougon, N., & Prêteux, F. 1991. Deformable markers: Mathematical morphology for active contour models control. *Pages 78–89 of: Image algebra and morphological image processing ii*. SPIE Proc., vol. 1568. Bellingham, WA: SPIE. 10

Rougon, N., & Prêteux, F. 1993. Directional adaptive deformable models for segmentation with application to 2D and 3D medical images. *Pages 193–207 of: Medical imaging 93: Image processing*. SPIE Proc., vol. 1898. 9

Sandor, S., & Leahy, R. 1995. Towards automatic labelling of the cerebral cortex using a deformable atlas model. *In:* [Bizais *et al.*, 1995]. 16, 17

Sapiro, G., Kimmel, R., & Caselles, V. 1995 (July). Object detection and measurements in medical images via geodesic deformable contours. *Pages 366–378 of: Vision geometry iv*. SPIE Proc., vol. 2573. 10, 23

Singh, A., von Kurowski, L., & Chiu, M.Y. 1993. Cardiac MR image segmentation using deformable models. *Pages 8–28 of: Biomedical image processing and biomedical visualization*. SPIE Proc., vol. 1905. Bellingham, WA: SPIE. 8, 17

Singh, A., Goldgof, D., & Terzopoulos, D. 1998. *Deformable models in medical image analysis*. Los Alamitos, CA: IEEE Computer Society. 3

Snell, J.W., Merickel, M.B., Ortega, J.M., Goble, J.C., Brookeman, J.R., & Kassell, N.F. 1995. Model-based boundary estimation of complex objects using hierarchical active surface templates. *Pattern recognition*, **28**(10), 1599–1609. 16

Staib, L.H., & Duncan, J.S. 1992a. Boundary finding with parametrically deformable models. *Ieee trans. on pattern analysis and machine intelligence*, **14**(11), 1061–1075. 13

Staib, L.H., & Duncan, J.S. 1992b. Deformable Fourier models for surface finding in 3D images. *Pages 90–104 of:* Robb, R.A. (ed), *Proc. second conf. on visualization in biomedical computing (vbc'92), chapel hill, nc, october*. SPIE Proc., vol. 1808. Bellingham, WA: SPIE. 12

Strang, G., & Nguyen, T. 1996. *Wavelets and filter banks*. Wellesley, MA: Wellesley-Cambridge Press. 22

Stytz, M., Frieder, G., & Frieder, O. 1991. Three-dimensional medical imaging: Algorithms and computer systems. *Acm computing surveys*, **23**(4), 421–499. 3

Subsol, G., Thirion, J.Ph., & Ayache, N. 1995. A general scheme for automatically building 3D morphometric anatomical atlases: Application to a skull atlas. *Pages 226–233 of: Proc. second international symp. on medical robotics and computer assisted surgery (mrcas'95), baltimore, md, november*. 16

Suri, J.S., Liu, K., Singh, S., Laxminarayan, S.N., Zeng, X., & Reden, L. 2002. Shape recovery algorithms using level sets in 2-D/3-D medical imagery: A state-of-the-art review. *Ieee transactions on information technology in biomedicine*, **6**(1), 8–28. 23

Székely, G., Kelemen, A., Brechbuhler, Ch., & Gerig, G. 1996. Segmentation of 2-D and 3-D objects from MRI volume data using constrained elastic deformations of flexible Fourier surface models. *Medical image analysis*, **1**(1). 13

Szeliski, R. 1990. Bayesian modeling of uncertainty in low-level vision. *International journal of computer vision*, **5**, 271–301. 7

Szeliski, R., Tonnesen, D., & Terzopoulos, D. 1993. Modeling surfaces of arbitrary topology with dynamic particles. *Pages 82–87 of: Proc. conf. computer vision and pattern recognition (cvpr'93), new york, ny, june*. 12

Tek, H., & Kimia, B. 1997. Volumetric segmentation of medical images by three-dimensional bubbles. *Computer vision and image understanding*, **65**(2), 246–258. 12

Terzopoulos, D. 1986a. *On matching deformable models to images*. Tech. rept. 60. Schlumberger Palo Alto Research. Reprinted in *Topical Meeting on Machine Vision,* Technical Digest Series, Vol. 12 (Optical Society of America, Washington, DC) 1987, 160-167. 4

Terzopoulos, D. 1986b. Regularization of inverse visual problems involving discontinuities. *Ieee trans. on pattern analysis and machine intelligence*, **8**(4), 413–424. 4

Terzopoulos, D., & Fleischer, K. 1988. Deformable models. *The visual computer*, **4**(6), 306–331. 4

Terzopoulos, D., & Metaxas, D. 1991. Dynamic 3D models with local and global deformations: Deformable superquadrics. *Ieee trans. on pattern analysis and machine intelligence*, **13**(7), 703–714. 13, 21

Terzopoulos, D., & Szeliski, R. 1992. Tracking with Kalman snakes. *Pages 3–20 of:* Blake, A., & Yuille, A. (eds), *Active vision*. Cambridge, MA: MIT Press. 8

Terzopoulos, D., Witkin, A., & Kass, M. 1988. Constraints on deformable models: Recovering 3D shape and nonrigid motion. *Artificial intelligence*, **36**(1), 91–123. 4, 9, 11, 16, 22

Thirion, J.P. 1994. Extremal points: Definition and application to 3D image registration. *Pages 587–592 of: Proc. conf. computer vision and pattern recognition (cvpr'94), seattle, wa, june.* 14

Thompson, P.M., & Toga, A.W. 1996-7. Detection, visualization and animation of abnormal anatomic structure with a deformable probabilistic brain atlas based on random vector field transformations. *Medical image analysis*, **1**(4), 271–294. 16

Troccaz, J., Grimson, E., & Mosges, R. (eds). 1997. *Proc. first joint conf. computer vision, virtual reality and robotics in medicine and medical robotics and computer-assisted surgery (cvrmed-mrcas'97), grenoble, france, march.* Lectures Notes in Computer Science, vol. 1205. Berlin, Germany: Springer-Verlag. 3, 26, 30, 31

Tsai, Richar, & Osher, Stanley. 2003. Level set methods and their applications in image science. *Communications of mathematical sciences*, **1**(4), 623–656. 23

Turk, G. 1992 (July). Re-tiling polygonal surfaces. *Pages 55–64 of: Computer graphics (proc. acm siggraph'92 conf.)*, vol. 26(2). 21

Ueda, N., & Mase, K. 1992. Tracking moving contours using energy-minimizing elastic contour models. *Pages 453–457 of:* Sandini, G. (ed), *Proc. second european conf. on computer vision (eccv'92), santa margherita ligure, italy, may.* Lectures Notes in Computer Science. Springer-Verlag. 9, 17

Vaillant, M., & Davatzikos, C. 1997. Mapping the cerebral sulci: Application to morphological analysis of the cortex and non-rigid registration. *In:* [Duncan & Gindi, 1997]. 16

Vasilescu, M., & Terzopoulos, D. 1992. Adaptive meshes and shells: Irregular triangulation, discontinuities and hierarchical subdivision. *Pages 829–832 of: Proc. conf. computer vision and pattern recognition (cvpr'92), urbana, il, june.* 22

Vemuri, B.C., & Radisavljevic, A. 1994. Multiresolution stochastic hybrid shape models with fractal priors. *Acm trans. on graphics*, **13**(2), 177–207. 13, 21, 22

Vemuri, B.C., Radisavljevic, A., & Leonard, C. 1993. Multiresolution 3D stochastic shape models for image segmentation. *Pages 62–76 of:* Colchester, A.C.F., & Hawkes, D.J. (eds), *Information processing in medical imaging: Proc. 13th int. conf. (ipmi'93), flagstaff, az, june.* Lectures Notes in Computer Science. Springer-Verlag. 13, 22

Wang, Y., & Staib, L.H. 1998. Elastic model based non-rigid registration incorporating statistical shape information. *In:* [Wells *et al.*, 1998]. 16

Waters, K. 1992. A physical model of facial tissue and muscle articulation derived from computer tomography data. *Pages 574–583 of:* Robb, R.A. (ed), *Proc. second conf. on visualization in biomedical computing (vbc'92), chapel hill, nc, october.* SPIE Proc., vol. 1808. Bellingham, WA: SPIE. 22

Wells, W., Colchester, A., & Delp, S. (eds). 1998. *Medical image computing and computer-assisted intervention: Proc. 1st int. conf. (miccai'98), cambridge, ma, usa, october.* Lectures Notes in Computer Science, vol. 1496. Berlin, Germany: Springer. 3, 22, 30, 34, 35

Whitaker, R. 1994. Volumetric deformable models: Active blobs. *In:* [Robb, 1994]. 10, 12, 23

Widrow, B. 1973. The rubber mask technique, part I. *Pattern recognition*, **5**(3), 175–211. 4

Witkin, A., Terzopoulos, D., & Kass, M. 1987. Signal matching through scale space. *International journal of computer vision*, **1**(2), 321–331. 16

Worring, M., Smeulders, A.W.M., Staib, L.H., & Duncan, J.S. 1996. Parameterized feasible boundaries in gradient vector fields. *Computer vision and image understanding*, **63**(1), 135–144. 13

Xu, C., & Prince, J.L. 1998. Snakes, shapes, and gradient vector flow. *Ieee transactions on image processing*, March, 359–369. 12

Yezzi, A., Kichenassamy, S., Kumar, A., Olver, P., & Tannenbaum, A. 1997. A geometric snake model for segmentation of medical imagery. *Ieee trans. on medical imaging*, **16**(2), 199–209. 10

Young, A., & Axel, L. 1992. Non-rigid wall motion using MR tagging. *Pages 399–404 of: Proc. conf. computer vision and pattern recognition (cvpr'92), urbana, il, june.* 20, 22

Young, A.A., Axel, L., Dougherty, L., Bogen, D.K., & Parenteau, C.S. 1993. Validation of tagging with MR imaging to estimate material deformation. *Radiology*, **188**, 101–108. 20

Young, A.A., Kraitchman, D.L., Dougherty, L., & Axel, L. 1995. Tracking and finite element analysis of stripe deformation in magnetic resonance tagging. *Ieee trans. on medical imaging*, **14**(3), 413–421. 20

Yuille, A.L., Hallinan, P.W., & Cohen, D.S. 1992. Feature extraction from faces using deformable templates. *International journal of computer vision*, **8**, 99–111. 13

Zeng, X., Staib, L.H., Schultz, R.T., & Duncan, J.S. 1998. Segmentation and measurement of the cortex from 3D MR images. *In:* [Wells *et al.*, 1998]. 12

Zienkiewicz, O.C., & Taylor, R.L. 1989. *The finite element method.* New York: McGraw-Hill. 6

Index

Deformable models, 1–35
- Accuracy, 22
- Active contour models, 4–7
- Active shape models, 14
- Autonomy vs control, 20–21
- Balloon, 11
- Compactness, 21
- Curve vs surface vs solid, 21–22
- Deformable curves, 8–10
- Deformable cylinders, 11
- Deformable organisms, 14
- Deformable surfaces, 11–12
- Discretization, 6–7
- Dynamic, 6
- Elastically deformable atlas, 16
- Energy minimizing, 4–5
- Eulerian, 23
- Finite elements, 6, 11, 20, 21
- Fourier representation, 12
- Generality vs specificity, 21
- Geometric coverage, 21
- Lagrange equations of motion, 6
- Lagrangian, 23
- Level set methods, 23
- Matching with, 14–16
- Mathematical foundations, 4–8
- Modal models, 18–20
- Motion analysis with, 16–20
- Motion tracking with, 16–20
- Nonrigid registration with, 14–16
- Numerical solution of, 6–7
- Oriented particle system, 12
- Prior knowledge, 12–14
- Probabilistic, 7–8
- Quantitative power, 22
- Robustness, 22
- Snakes, 4–9
- Splines, 4, 7, 11, 13, 16, 21
- T-snakes, 9, 12, 23
- T-surfaces, 12, 23
- Topological flexibility, 21